INFLUENCE OF HYDROGEN ON DELAYED FRACTURE IN HIGH MANGANESE TWINNING INDUCED PLASTICITY (TWIP) STEELS AND OTHER ADVANCED HIGH STRENGTH STEELS (AHSS)

A DISSERTATION

Submitted in partial fulfillment of the

requirements for the award of the degree

of

MASTER OF TECHNOLOGY

in

METALLURGICAL AND MATERIALS ENGINEERING

(With specialization in Industrial Metallurgy)

BY

AJEET SINGH RAJPUT

DEPARTMENT OF METALLURGICAL AND MATERIALS ENGINEERING

INDIAN INSTITUTE OF TECHNOLOGY ROORKEE

ROORKEE – 247667, INDIA

MAY, 2016

CANDIDATE'S DECLARATION

I hereby declare that the proposed work presented in this dissertation entitled **"Influence of hydrogen on delayed fracture in high manganese Twinning Induced Plasticity (TWIP) steels and other advanced high strength steels (AHSS)**" in partial fulfillment of the requirements for the award of the degree of **Master of Technology** in **Metallurgical and Materials Engineering** with specialization in Industrial Metallurgy, submitted in the **Department of Metallurgy and Materials Engineering, Indian Institute of Technology Roorkee** is an authentic record of my own work carried out during the period from July 2015 to May 2016 under the supervision of **Dr. P. K. Ghosh**, Professor, Department of Metallurgical and Materials Engineering, Indian Institute of Technology Roorkee, India.

The matter presented in this dissertation has not been submitted by me for the award of any other degree.

Dated:

Place: Roorkee **Ajeet Singh Rajput**

CERTIFICATE

This is to certify that the above statement made by the candidate is correct to the best of my knowledge and belief.

Dr. P. K. Ghosh
Professor
Department of Metallurgical & Materials Engineering
Indian Institute of Technology, Roorkee
Roorkee-247667 (INDIA)

CANDIDATE'S DECLARATION

I hereby declare that the proposed work presented in this dissertation entitled **"Influence of hydrogen on delayed fracture in high manganese Twinning Induced Plasticity (TWIP) steels and other advanced high strength steels (AHSS)"** in partial fulfillment of the requirements for the award of the degree of **Master of Technology** in **Metallurgical and Materials Engineering** with specialization in Industrial Metallurgy, submitted in the **Department of Metallurgy and Materials Engineering, Indian Institute of Technology Roorkee** is an authentic record of my own work carried out during the period from July 2015 to May 2016 under the supervision of **Dr. P. K. Ghosh**, Professor, Department of Metallurgy and Materials Engineering, Indian Institute of Technology Roorkee, India and **Univ.-Prof. Dr.-Ing. Wolfgang Bleck,** Chair and Department of Ferrous Metallurgy, Professor, Institute of Ferrous Metallurgy, Rheinisch-Westfälische Technische Hochschule Aachen, Germany.

The matter presented in this dissertation has not been submitted by me for the award of any other degree.

Dated:

Place: Roorkee

Ajeet Singh Rajput

CERTIFICATE

This is to certify that the above statement made by the candidate is correct to the best of my knowledge and belief.

INSTITUT FÜR EISENHÜTTENKUNDE
Der Rhein.-Westf. Techn. Hochschule Aachen

(Prof. Dr.-Ing. Wolfgang Bleck)
Institut für Eisenhüttenkunde
der Rhein.-Westf. Technischen Hochschule
Intzestraße 1
52072 Aachen

ACKNOWLEDEMENTS

I consider myself very fortunate to receive the unique opportunity to conduct my project work at two prime institutions of two great countries and would like to thank **DAAD** for making it happen through **DAAD-IIT Master's Sandwich Program for students at the IITs**. I sincerely acknowledge everyone at **Indian Institute of Technology, Roorkee** and **Rheinisch-Westfälische Technische Hochschule Aachen** from whom I received help, support and guidance of any kind.

I would like to express my sincere gratitude and indebtedness to my supervisor **Prof. Dr. P. K. Ghosh**, Department of Metallurgical and Materials Engineering, Indian Institute of Technology, Roorkee, for their encouragement and scholastic guidance all through the tenure of this project work.

I express my sincere thanks to **Univ.-Prof. Dr.-Ing. Wolfgang Bleck,** Chair and Department of Ferrous Metallurgy**,** for hosting me at Rheinisch-Westfälische Technische Hochschule, Aachen, Germany and being a guiding light all along. I am also grateful to **Mr. Manjunatha Madivala** for his invaluable support and supervision during my research here.

I would also like to thank my respected Head of the Department **Prof S.K. Nath** for providing all the facilities required to carry out the work. I would also like to thank **Dr. Vikram V. Dabhade** for believing in me and recommending for the fellowship.

Besides, I would like to thank all the friends I met in Aachen. I would say it is fabulous that we spent some time together in Germany.

Last but not the least I would like to thank my family and friends for their continuous affection and moral support throughout the project.

Ajeet Singh Rajput

ABSTRACT

Delayed fracture (DF) behaviour by presence of hydrogen is a non–negligible obstacle for fully application of excellent formability of advanced high strength steel (AHSS) such as high manganese Twinning Induced Plasticity (TWIP) steel, Transformation Induced Plasticity (TRIP) steel and Dual Phase (DP) steel. TWIP steels have austenitic structure and are a type of specific AHSS which show higher strength and ductility than that of other AHSS of ferritic and martensitic structure (i.e. DP and TRIP). The current work investigated the influence of hydrogen on delayed fracture behaviour in high manganese TWIP steels and other advanced high strength steel (AHSS) by carrying out slow strain rate test (SSRT) and deep drawing test (DDT). Slow strain rate test (SSRT) were employed on both tensile and notched tensile specimens of investigated materials to evaluate the influence of diffusible hydrogen on the hydrogen embrittlement effect (by tensile specimens) and influence of complex stress state (by notched tensile specimens) of the high manganese TWIP steel and other AHSS. Deep drawing test (DDT) was conducted on round blanks of investigated materials to investigate the effect of diffusible hydrogen on the delayed fracture behaviour of high manganese TWIP steel and other AHSS. By addition of Aluminium (Al) as an alloying element in high manganese TWIP steel such as X30MnAl22-1 showed postponed initiation of mechanical twinning upon deformation than X60Mn22. Since Al increases the stacking fault energy of austenite, the tendency for mechanical twinning is decreased, and the formation of deformation-induced martensite eliminated. It explored benefit of homogeneously dispersed fine Aluminium Nitrides as hydrogen traps that acts as an obstacle for diffusion of hydrogen in steel. Hydrogen–dislocation interaction is mostly increased at low strain rate (in SSRT) and high tri-axial stressed condition (in DDT).The fracture mechanisms in the investigated materials were identified by observing the fracture surfaces in scanning electron microscopy (SEM).

CONTENTS

LIST OF FIGURES

LIST OF TABLES

ABBREVIATIONS AND SYMBOLS

AHSS	Advanced High Strength Steel
BCC	Body centered cubic
BHF	Blank Holder Force, in kN
DC	Delayed Cracking
DDT	Deep Drawing Test
DF	Delayed Fracture
DF-S	Delayed Fracture Susceptibility
DP	Dual Phase
DR	Drawing Ratio
FCC	Face Centered Cubic
FPZ	Fracture Process Zone
HAC	Hydrogen Assisted Cracking
HCP	Hexagonal Close Packed
HPT	Hydrogen Pressure Theory
HEAC	Hydrogen Environment Assisted Cracking
HE	Hydrogen Embrittlement
HEDE	Hydrogen Enhanced Decohesion
HE-S	Hydrogen Embrittlement Susceptibility
HELP	Hydrogen Enhanced Localized Plasticity
High manganese TWIP steel	High Manganese Steel
HTHA	High Temperature Hydrogen Attack
LTHA	Low Temperature Hydrogen Attack
PV	Punch Velocity, in mm/min
QTT	Quasi-static Tensile Test
SEM	Scanning Electron Microscope
SF	Stacking Fault
SFE	Stacking Fault Energy
SSRT	Slow Strain Rate Test
TRIP	Transformation-Induced Plasticity
TWIP	Twinning-Induced Plasticity

α		Ferrite phase
ά		Alpha martensite phase
D	m^2/s	Lattice diffusion coefficient
D_0	m^2/s	Pre-exponential factor
ε		Epsilon martensite phase
$\varepsilon_{H\ charged}$		Uniform elongation of H charged SSRT specimen
$\varepsilon_{uncharged}$		Uniform elongation of H uncharged SSRT specimen
γ		Austenite phase
γ_{SFE}	mJ/m^2	Stacking Fault Energy
J		Flux density of hydrogen diffusion
Q	kJ/mol	Activation energy for diffusion
R	J/(mol.K)	Universal gas constant (8.314×10^{-3} j/(mol.k))
R	m	Radius of element
$\sigma_{H\ charged}$	MPa	Tensile stress of H charged SSRT specimen
$\sigma_{uncharged}$	MPa	Tensile stress of H uncharged SSRT specimen
$\Phi_{specimen}$	mm	Diameter of DDT specimen
Φ_{punch}	mm	Diameter of DDT drawing punch

CHAPTER 1: INTRODUCTION

Advanced high strength steels (AHSS) have been generated because of the huge demands of excellent mechanical properties, high recycling efficiency and lightweight. Now a days the requirement of creating light-weight and high-safety vehicles leads to urgent demand for ultra-high strength structural materials. Many investigations have been conducted about the first-generation AHSS such as dual phase (DP), complex phase (CP) and transformation induced plasticity (TRIP) steels. The first-generation AHSS has the high strength of above 700 MPa at the expense of uniform ductility, resulting in the limited strength–ductility balance of about 20,000 MPa%.

The second generation AHSS are High Mn austenitic steels such as Hadfield, TRIP, twinning-induced plasticity (TWIP) and shear/ micro-band induced plasticity (SBIP/MBIP) steels. These steels have an excellent combination of high strength of above 800 MPa and large uniform ductility of over 60% because of the high strain hardening rate by the formation of martensite, twins, or dislocation bands during the plastic deformation. The strength–ductility balance of about 60,000 MPa% of the second-generation AHSS is three times higher than that of the first-generation AHSS. Especially, high manganese TWIP steel has been highlighted because of excellent mechanical properties. High manganese steels (High manganese TWIP steel) showing TWIP effect and other AHSS are attractive for various industrial applications. They are not too costly and have excellent strength-ductility combinations compared with conventional carbon steels. These materials are necessary especially to produce complicated deep drawn parts with reduced welding applications or post processing procedures. **Figure 1.1,** shows excellent strength-ductility combinations of these materials compared with conventional carbon steels, due to the merits these materials use in automotive, aerospace or marine industries [1].

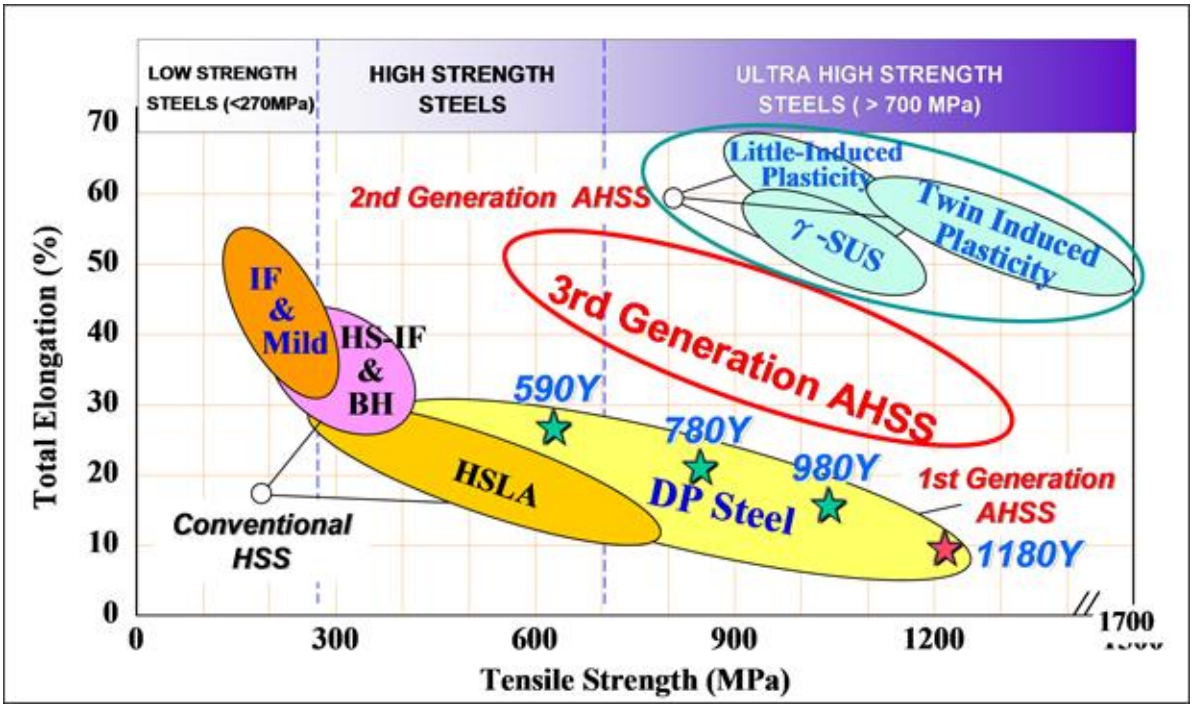

Figure 1.1: The tensile strength and total elongation relationship for various structural steels.

However, mechanical degradation of structural materials by hydrogen is a serious problem that has received increasing attention from the last sixty years. The risk of delayed fracture, a phenomenon in which the deformed materials suddenly fails under external stress or residual stress, increases with the increasing strength of high strength steels. This undesirable effect results from hydrogen introduced into the steel from metallurgical process or their service environment. Intensive investigations have been conducted on studying the hydrogen-microstructure interactions upon plastic deformation [2-4]. Compared to other carbon steels at the same stressed condition, ferritic steels generally have high susceptibility to Hydrogen Embrittlement (HE), since hydrogen diffusivity in ferritic steels is several orders higher than that in austenitic steels. However, High manganese TWIP steel and other AHSS are considered to be particularly prone to HE due to combined effect of strain induced martensite transformation or mechanical twinning with high strength level. It is well known hydrogen assisted delayed fracture is always very close related to the brittle martensite phase in the TRIP steel. Some literatures described the high delayed fracture susceptibility due to the presence of hydrogen in the high manganese TWIP steels, in which the adding of 1-3% weight Al as alloying element could successfully enhance delayed fracture resistance [5-7]. Although the effect of Al addition in raising the stacking fault energy in TWIP steels and

delaying the mechanical twinning had been elucidated [5,8-9]. However, the mechanisms of preventing delayed fracture by Al addition have been not thoroughly explored.

Many studies have been carried out and several mechanisms have been proposed on how hydrogen affects structural materials from a long time. However, the mechanism of the delayed fracture is still not exactly clear, according to previous research work, there are facts showing that the delayed fracture is influenced by microstructure, residual stress effect in the specimen after deformation and so on. The mechanisms of DF are very complex as several factors may influence and interact with each other, therefore, a deep-through investigation is required for the respective influencing factors on the delayed fracture behaviour.

The current work focuses on two main aspects in high manganese TWIP steel and other AHSS: chemical composition and microstructure, which influence DF behaviour. By applying electro-chemical hydrogen charging, slow strain rate test and deep drawing test, the mechanical properties and DF behaviour as functions of hydrogen content are quantified. Fracture surface is identified with scanning electron microscopy (SEM) technique which helps to understand the damage mechanisms relating to hydrogen and microstructure. The study of environmental influences on DF behaviour are neglected in this work, because corrosion during material-environmental interaction may lead to more complex situations and fade the main aim of this work.

CHAPTER 2: LITERATURE REVIEW

2.1 Types of advanced high strength steels (AHSS)

2.1.1 Twinning-Induced Plasticity (TWIP) steel

Twinning-Induced Plasticity (TWIP) steel is newly developed high manganese steel with a fully austenitic phase at room temperature. The deformation twins will appear in TWIP steel when an external load is applied, which leads to an outstanding combination of ductility and strength [10-12]. The ultimate tensile strength can be more than 800 MPa while elongation is upto 65%. The dramatic performance provides a new thinking for the design of car-body material [11-14]. This is the main reason TWIP steels are so attractive in recent researches of automobile industry.

Twinning-Induced Plasticity (TWIP) mechanisms

The Fe-Mn-C steels generally have relatively low stacking fault energy (SFE) at room temperature. In austenitic steels, twinning occurs within the stacking fault energy range 18-45 mJ/m^2 upon plastic deformation. The low stacking fault energy value will promote the mechanical twinning competition with the gliding along with strain. The deformation-induced twins moderately decrease the effective glide distance of dislocations, which results in the effect of "Dynamic Hall-Petch". **Figure 2.1** [14] showed the decreased dislocation mean free path due to deformation twins reduces dislocation glide distance, leading to a high value of the instantaneous hardening rate, which is like the effect of grain refinement. The resultant twin boundaries act as grain boundaries and strengthen the steel. Mechanical twinning produces hardening effect that is known as twinning-induced plasticity (TWIP) effect.

From some certain observations, it is understood that not only crystallographic orientation that has a strong influence on deformation twinning, but the grain size also plays an main role [15]. However, there are not many literatures on this topic.

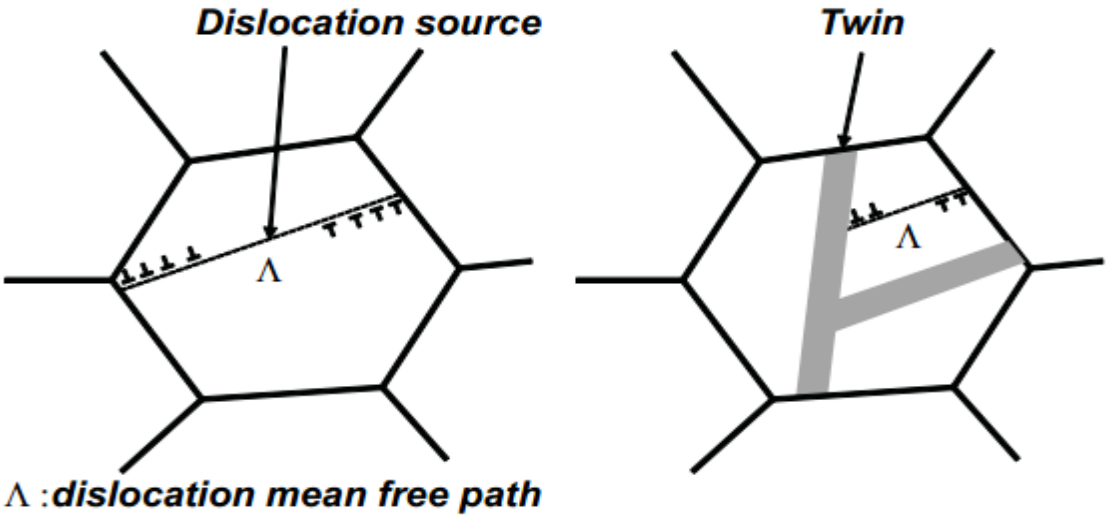

Figure 2.1: Sketching of the effect of "dynamic Hall-Petch". Formation of mechanical twins happens due to the low SFE, reducing the effective glide distance of dislocations [14].

Main alloying elements

Carbon is most effective austenite stabilizer. Its main functions in steel are improving the formation of fully austenite microstructure and solution strengthening, in order to ensure high mechanical properties of steels [16].

The value of SFE will increase with increasing carbon content, so that the transformation of ε-martensite will be impeded. In the high Mn content Fe-Mn alloys, adding of carbon can lead to a larger austenitic phase and improve the mechanical properties. But excess amount of carbon also causes many problems, such as the ductility of steel decreases significantly. So in the traditional TWIP steel, the carbon content is usually relatively low [17].

Manganese is an important alloying element in TWIP steel, which can enlarge the austenite phase and strongly stabilize the austenite microstructure [16]. The value of SFE will also increase with increasing Mn content like carbon. The steel with a high SFE prefers twinning induced plasticity (TWIP) effect instead of transformation induced plasticity (TRIP) effect. But the ductility at low temperature will decrease if the manganese content is higher than 35%. In the high Mn Fe-Mn-Al-Si TWIP/TRIP steels, the manganese content is in range of approximate 15 to 30% [18].

Aluminium is also an important alloying element, which plays a role in deoxygenating, resistance of oxidation, resistance of corrosion and solution strengthening. The addition of Al can improve the processability, strain hardening rate and the ductility at low temperature of the steels [19]. Al can increase the SFE of the steel significantly, which is good for achieving the TWIP effect. Kim et al. [14] also have observed that, the addition of Al in the TWIP steels has a good resistance of the delayed fracture. However, the over content of Al lead to bad casting properties. So addition of proper amount of Al is a matter of concern.

2.1.2 Transformation-Induced Plasticity (TRIP) steel

TRIP steel is an advanced high-strength steel mostly used in the automotive industry. TRIP is an acronym used for "Transformation Induced Plasticity" steel having good combination of strength and ductility.

Microstructure

TRIP steel has a microstructure consisting of retained austenite in a ferrite matrix. As well as it also consists hard phases like bainite and martensite. The higher carbon and silicon levels in TRIP steels lead to significant volume fractions of retained austenite in the resulting final microstructure.

Higher contents of carbon present in TRIP steels than dual phase steels to gain adequate carbon quantity for stabilization of the retained austenite phase to below surrounding temperature. Greater levels of silicon or aluminium speed up the ferrite/bainite formation. They are also added to avoid carbide formation in the bainite region.

Metallurgical properties

At the time of plastic deformation and straining, transformation of the retained austenite phase into martensite happened. Thus increasing the strength by the phenomenon of strain hardening. Strength and ductility are increased by this transformation. High strain hardening capacity and high mechanical strength provide these steels excellent energy absorption capacity.

Effect of alloying elements

The amount of carbon controls the strain level at which the retained austenite begins to transform in martensite. At smaller carbon contents, the retained austenite begins to transform almost immediately upon deformation, enhancing the work hardening rate and formability. At greater carbon levels, the retained austenite is more stable and begins to transform only at strain levels beyond those produced during forming.

2.1.3 Dual Phase (DP) steel

Dual Phase (DP) steel offers an outstanding combination of strength and ductility because of their microstructure, in which a hard martensitic phase is dispersed in a soft ferritic matrix. These steels have high strain hardenability.

Microstructure

Dual phase (DP) steel is an advanced high-strength steel that has a ferritic and martensitic microstructure. The microstructure consisting of a soft ferrite matrix containing martensite islands as the secondary phase (martensite increases the tensile strength). DP steel have high ultimate tensile strength (UTS, because of the martensite) combined with low initial yielding stress (provided by the ferrite phase), high strain hardening at early-stage and macroscopically homogeneous plastic flow. These features make DP steel as ideal material for automotive-related sheet forming operations.

Effect of alloying elements

DP steel typically contain 0.06–0.15 wt% C (to strengthen the martensite) and 1.5-3% Mn (to provide solid solution strengthening in ferrite), both are austenite stabilizer, Cr & Mo (to retard pearlite or bainite formation), Si (to promote ferrite transformation), V and Nb (to strengthening of precipitates and microstructure refinement).

2.2 Hydrogen in steels

Hydrogen is the most abundant element in the universe. It is safe and clean fuel gas of high calorific value, available in enough quantity by the electrolysis of water. Hydrogen is the lightest element having atomic structure of one proton and a single electron and it is diatomic molecular gas H_2 in neutral state. The diatomic hydrogen molecule is too large to enter the surface of a solid metal, and must be dissociated into single atom to readily enter into metal surface.

2.2.1 Sources of hydrogen in steel

Many hydrogen sources present throughout steel production and in service. The sources of hydrogen in steel are the following: gaseous hydrogen, discharge of atomic hydrogen by the iron-water, decomposition of water molecules, corrosion and electrolytic processes including a cathodic reaction.

Hydrogen is formed during pickling in mineral acids, cathodic electrolytic cleaning, cathodic polarization protection, and zinc or cadmium plating. In all cases it happens due to a cathodic reduction. In case of pickling, the anodic counter reaction is dissolution of metal and occurs at the same location as evolution of hydrogen. The cathodic evolution of hydrogen from aqueous electrolytes is happened in several successive steps. Depending upon the electrolyte, the overall hydrogen evolution reaction (HER) can be written:

In acid medium $$2H_3O^+ + 2e^- \rightarrow H_2 \uparrow + 2H_2O \quad (2\text{-}1)$$

In alkaline medium $$2H_2O + 2e^- \rightarrow H_2 \uparrow + 2OH^- \quad (2\text{-}2)$$

It is now generally accepted that two successive steps are necessary to the overall HER mechanism. The first step consists in either discharge of hydrated protons (in acid medium):

$$H_3O^+ + M + e^- \rightarrow MH_{ads} + H_2O \quad (2\text{-}3)$$

Or electrolysis of water (in alkaline medium):

$$H_2O + M + e^- \rightarrow MH_{ads} + OH^- \quad (2\text{-}4)$$

Where MH_{ads} represents hydrogen atom absorbed on the metal surface.

The absorbed hydrogen atom can react to form molecular hydrogen according to Tafel reaction (2-5) or Heyrovsky reaction (2-6). Molecular hydrogen is generated and released from an electrolyte as a gas bubble.

$$H_{ads} + H_{ads} \rightarrow H_2\uparrow \quad (2\text{-}5)$$

$$H_{ads} + \mathrm{H}^+ + e^- \rightarrow H_2\uparrow \quad (2\text{-}6)$$

Alternatively, it diffuses into a bulk of material as absorbed hydrogen (H_{abs}):

$$H_{ads} \rightarrow H_{abs} \quad (2\text{-}7)$$

The rate of hydrogen absorption can be greatly affected by surface adsorbates called recombination poisons. The presence of poisons on steel-electrolyte interface enhances hydrogen absorption by creating a blocking action on recombination of hydrogen. The poisons consist of the following elements and certain their compounds: S, P, As, Se, Sn, Sb, Te. When hydrogen recombination is reduced, the ability of atomic hydrogen to enter steel is promoted [2,20].

Corrosion of marine constructions is retarded by coatings and cathodic protection. In steel making process, hydrogen is reserved in the melt from the damped charged materials, slag, new refractory linings, hydrocarbon fuels and etc. The effect of hydrogen uptake in liquid steel is the formation of flake, which may appear for a long time after solidification, rolling or forging. In welding hydrogen absorption occur from damp fluxes, hydrocarbon preheating gases, rust or grease on the steels.

2.2.2 Sites and traps for hydrogen

Various crystal defects have different interactions with hydrogen, lead to local hydrogen enrichment, which is called “trapping”. Solute hydrogen occupies and diffuses between interstitial sites in metals, and can be trapped at other sites (i.e. occupy lower potential-energy sites). These other sites are: some solute atoms, mono-vacancies and vacancy clusters, dislocation cores and strain fields, grain boundaries (containing prior-austenite grain boundaries in martensitic steels), precipitate/matrix interfaces and strain fields around

precipitates, inclusion/matrix interfaces, voids and internal cracks. Generally hydrogen atoms distribute inhomogeneously in materials.

Hydrogen trap sites can be of two types: reversible and irreversible. The reversible or diffusible trapping sites are associated with the low activation energy for detrapping, such as grain boundaries [21], dislocations [22], and coherent carbide interfaces [23]. Hydrogen embrittlement (HE) is mainly caused by hydrogen at these diffusible trapping sites. The irreversible or non-diffusible trapping sites are associated with the high energy barriers for detrapping, such as inclusions [24], voids [25] and incoherent carbide interfaces [23]. These non-diffusible trapping sites are not responsible for HE. The irreversible traps have much higher binding energies than reversible traps. Due to the low binding energy, hydrogen in reversible traps can be easily reactivated. They are likely to participate in any HE process which causes more damage and accelerate failure. Hydrogen atoms trapped in irreversible trap sites are released only at very high temperatures and do not take part to HE at surrounding temperature. From the literature reviews it is observed that the reversible hydrogen traps have the binding energy below 30-40 kJ/mol and the irreversible traps have extremely high binding energy. Aucouturier et. al have observed high hydrogen concentrations in austenitic steels at the intersections of slip lines and grain boundaries and in ε and ά- martensite [26]. They used thermal desorption analysis at different heating rates. Their calculation indicated that the twinning boundaries in high manganese steels are irreversible hydrogen traps. Once, trapped hydrogen atoms will have a longer residence time until the thermal kinetics of hydrogen atoms are raised by heating. As a result, trapping reduces hydrogen diffusivity and raises local hydrogen enrichment, where cracks locally initiate.

2.2.3 Hydrogen solubility and hydrogen diffusivity

Hydrogen atoms prefer to occupy the octahedral interstitial sites in FCC microstructure and tetrahedral interstitial sites in BCC microstructure. Hydrogen atoms with radius of 0.32×10^{-10} m cause much less lattice distortion in comparison with the interstitial elements C ($r = 0.77\times10^{-10}$ m) and N ($r = 0.75\times 10^{-10}$ m). **Table 2.1,** showed number of octahedral and tetrahedral interstitial sites in FCC and BCC microstructures and the maximum spacing for foreign atoms. Hydrogen has higher solubility in FCC γ-iron than in BCC α-iron due to

the easiness to expand octahedral sites. Hydrogen solubility is also very high in HCP ε-iron [27,28]. As the temperature increases, hydrogen solubility increases in both phases.

Table 2.1: Number of interstitial sites in FCC and BCC microstructures and the maximum spacing for foreign atoms [29]

Crystal Structure	Octahedral interstices		Tetrahedral interstices	
	Number	Maximum Spacing r	Number	Maximum Spacing r
BCC	6	0.19×10^{-10}m	12	0.36×10^{-10}m
FCC	4	0.53×10^{-10}m	8	0.28×10^{-10}m
HCP	4	0.53×10^{-10}m	8	0.28×10^{-10}m

Commercial steels have very high hydrogen solubility in compare to ideal lattice, because various lattice defects increase hydrogen solubility by working as hydrogen trapping sites. The various alloying elements effect hydrogen solubility in molten iron. The elements Cr, Mn, Ni, Nb, N may increase hydrogen solubility, whereas, the elements Al, Co, Mo, B, Si, C would decrease hydrogen solubility.

According to Fick's first law, the diffusion flux density J is proportional to the concentration gradient

$$J = -D.grad\ C = -D\frac{dC}{dx} \tag{2-8}$$

$$D = D_0.\exp\left(-\frac{Q}{RT}\right) \tag{2-9}$$

Where D refers as the hydrogen diffusion coefficient in steel, C stands for the hydrogen concentration, Q stands for activation energy and T stands for temperature. Equation (2-9) is called Arrhenius equation. D_0 is a pre-exponential factor with the unit of m^2/s and R is the universal gas constant (8.314×10^{-3} j/(mol-k)).

Concentration gradient of hydrogen is related to the chemical potential, the diffusion of hydrogen can be treated as driven by the gradients in the chemical potential of hydrogen in solid solution from distant areas towards the crack tip. Different crystal structures have different values of activation energy for hydrogen diffusion. At room temperature, hydrogen diffusion coefficient in BCC structure is several orders higher than that in FCC or HCP structure.

Hydrogen diffuses through the lattice due to hydrogen concentration gradient, temperature gradient and hydrostatic stress fields gradient. Hydrogen can be transported more rapidly by mobile dislocations than by lattice diffusion when hydrogen is present at dislocation cores or at atmosphere around dislocations. Dislocation transport of hydrogen may be important in moving hydrogen form grain interiors to grain boundaries, thereby promoting intergranular fracture. Hydrogen may also diffuse more rapidly along grain boundaries as compared to the lattice in some cases, but if there is a higher trap density at boundaries than anywhere, then grain boundary diffusion of hydrogen could be slower than through the lattice.

Alloying elements such as Ni, Cr, C, Ti reduce hydrogen diffusivity. In the opposite, hydrogen concentration gradient, temperature gradient, elastic stress gradient act as the driving force for hydrogen diffusion.

2.2.4 Types of damage due to hydrogen

Hydrogen damage is the name given to a large number of metal degradation processes due to interaction with hydrogen. Hydrogen is legendary for its ability to harm the ductility and toughness of steels and for its role in static failure, i.e. unpredicted failure after a component has been in service for a period well below its design life. Hydrogen damage can be divided into two main categories: Internal Hydrogen Assisted Cracking (IHAC) and Hydrogen Environment Assisted Cracking (HEAC) [30,31]. Both internal hydrogen assisted cracking (IHAC) and hydrogen environment assisted cracking (HEAC) restrict the performance of most modern structural alloys, and confound prognosis of component safety, durability and capability. IHAC and HEAC are distinguished by the source of the offending H supplied to the crack tip fracture process zone (FPZ), but otherwise share common aspects.

Internal Hydrogen Assisted Cracking (IHAC)

Hydrogen in atomic form can be introduced globally throughout the microstructure by manufacturing processes (e.g. welding, casting, surface-chemical cleaning, electrochemical machining, electroplating, and heat treatment) and by environmental exposure (e.g., cathodic electrochemical reactions at low temperatures and exposure to gaseous hydrogen at elevated temperatures). Subcritical crack growth occurs when the hydrogen charged metal is subsequently stressed. Loading causes a redistribution of dissolved hydrogen from the

surrounding microstructure to the crack tip process zone to enhance crack growth. Stress is not essential during hydrogen uptake, and environmental hydrogen production at the crack tip during stress is not significant as the loading environment is typically benign. IHAC is designed to be the degradation behaviour of pre-existing hydrogen in the material in combination with external or residual stresses. In some situations, even no external stress is present, the fracture process can take place under the drive force of residual stress. The fracture initiation process does not necessarily need aggressive environment, and is characterized for unpredicted incubation period. It is also called as Delayed Fracture (DF) or Delayed Cracking (DC).

IHAC is really an important issue that should be carefully considered during designing and application of high strength steels. There is possibility of DF in austenitic steels because austenitic microstructure allows high hydrogen solubility which act as a source for internal hydrogen.

Hydrogen Environment Assisted Cracking (HEAC)

HEAC involves the combined action of chemical reaction and mechanical loading. It is related to the aggressive atmosphere or aqueous solutions from the environment. Atomic hydrogen is produced predominantly on clean crack surfaces localized near to the tip, followed by H uptake into the crack tip FPZ and lead to embrittlement. Atomic hydrogen (H) is formed by dissociative chemical adsorption for H_2, chemical reactions for gases such as water vapour or H_2S, or electrochemical cathodic reactions for alkaline or acidic electrolytes. Once produced, the H diffuses ahead of the crack tip into the FPZ to influence damage. Electrochemical reactions resulting in metal dissolution and passive film formation can take place at the crack tip, concurrent with H production, to affect crack growth.

The above discussed both hydrogen degradation processes normally take place at ambient temperature, related to Low Temperature Hydrogen Attack (LTHA). Hydrogen induced damage includes many forms of degradation of metals caused by exposure to liquid or gas environments which cause absorption of hydrogen the metals to cause degradation in mechanical properties. Formation of blisters, internal cracks, voids in steels and hydrogen embrittlement are the examples of hydrogen induced damage. Hydrogen solubility in molten metal is much higher than in the solid condition. This hydrogen loading is reversible to a

great extent, because it is caused mainly due to presence of the hydrogen in the interstitial lattice sites. The fracture surface normally shows transgranular fracture feature.

When the hydrogen attack occur at high temperature, normally above $200^{\circ}C$, is called High Temperature Hydrogen Attack (HTHA). It is a surface decarburization process and chemical reaction with hydrogen. In HTHA, second phase formation takes place by the solute hydrogen and it is an elevated temperature phenomenon. Hydrogen solubility in α-Fe is ver less. Similarly, the solubility of carbon in α-Fe is very small. However, if two are present they can react together and form methane at a suitable elevated temperature.

$$C + 2H_2 \rightarrow CH_4 \qquad (2\text{-}10)$$

The reaction occurs at grain boundaries, where methane gas exerts internal pressure and forms fissures or elongated pores on metal. The fracture surface normally shows intergranular fracture feature. This phenomenon was observed in the petrochemical industries and synthetic ammonia industries, where equipment remain in contact with hydrogen at high temperatures.

2.2.5 Mechanisms related to hydrogen induced delayed fracture

Despite extensive study, the mechanisms of hydrogen embrittlement (HE) and delayed fracture (DF) are still remained unclear. Several mechanisms have evolved to clear the role of hydrogen in material degradation, each of which is based on set of experimental observations and strong personal views. The fundamental mechanisms for hydrogen embrittlement in metals have been extensively reviewed [32,33,34,35,36]. First time HE in steels was seen in pipeline industry and hydrogen storage suppliers, where the structural steels had to face high hydrogen pressure. Zapffe and Sims firstly proposed the Hydrogen Pressure Theory (HPT) based on assumption that precipitation of molecular hydrogen at internal defects (non-metallic inclusions, voids) generates high internal pressure. This pressure is added to applied stress and hence lowers the apparent fracture stress [37].

The stress induced hydride formation and fracture mechanism is one of the well known HE mechanisms with extensive experimental and theoretical support [33,38,39,40]. A mechanism based on formation and fracture of hydrides at crack tips was first given by Westlake in 1969

[41]. The basic mechanism consists of (i) hydrogen diffusion to regions of large hydrostatic stress ahead of cracks (ii) nucleation-growth of a hydride phase (iii) fracture of the hydride when it reaches a critical size (iv) arresting of crack at the hydride-matrix interface. A hydride formation mechanism only occurs at certain temperature and strain rate range where hydrogen got time to diffuse to regions ahead of crack tips only at temperatures where the hydride phase is stable and brittle [42,43]. A hydride mechanism is generally seen certain materials such as V, Ti, Zr, Nb and Ta because they have strong thermodynamic driving force for hydride formation and they form brittle hydrides. However, it is very difficult to form hydrides in Fe-based alloys in the referred conditions. Thus, the hydrides formation would not be a clarification for HE in steels [44].

Many researchers assigned delayed fracture as a type of internal reversible hydrogen embrittlement. To study the hydrogen-dislocation interactions upon plastic deformation, many experiments have been performed. In previous research data related to hydrogen induced delayed fracture and related mechanisms have been developed. Many materials show macroscopic reduction in ductility and brittle failure mode due to hydrogen present in material. Different mechanisms have been proposed to describe brittle fracture. However, some fractographic examinations with high resolution techniques revealed that HE is always associated with localized plasticity at the crack tip, showing ductile failure mode [45]. To explain hydrogen-dislocation interactions, two mechanisms have been proposed: Hydrogen Enhanced Localized Plasticity (HELP) and Hydrogen Enhanced Decohesion (HEDE).

Hydrogen Enhanced Localized Plasticity (HELP)

Absorption of hydrogen and its solid solution increases the ease of dislocation generation or motion, or both. Mechanism related to this, first proposed by Beachem and developed by Brinbaum et al. The HELP model proposed that the presence of hydrogen in solid solution decreases the barriers to dislocation motion hence increasing the amount of deformation that occurs in a localized region adjacent to the crack surface. This HELP has been attributed to the presence of a hydrogen atmosphere around dislocations which shields its interaction with dislocations, solute atoms etc. However, this mechanism suggests that the fracture process is started by a highly localized plastic failure at the microscopic level, the embrittlement takes place macroscopically due to the reduction in ductility during a tensile test. Hydrogen diffusion to local regions ahead of crack tips is required for working of the HELP mechanism

for both IHE and HEE. Cracks path could be transgranular or intergranular depending on the presence of locally high hydrogen concentrations within grain interiors or adjacent to grain boundaries.

High resolution fractography of hydrogen embrittled metals, such as Ni and Fe, show extensive plastic deformation localized along the fracture surfaces [46,47]. Principle in the HELP mechanism is the shielding of elastic interactions between dislocations and obstacles due to the hydrogen solutes. Reduction of the interaction energies between elastic stress centres results in enhanced dislocation mobility. This phenomenon is supported by strong experimental evidence and was observed in FCC, BCC and HCP systems. The local dislocation movement can take place at low levels of shearing stress in the presence of hydrogen, leading in increased amount of deformation that occurs in a localized region adjacent to the fracture surface, such as crack tips. The explanation can be hydrogen entry is facilitated by the slip process, stress enhances hydrogen agglomeration [48]. Due to sliding localization, micro cracks occur by the formation of micro pores and shearing action. Nagumo et al. experimentally showed that hydrogen enhanced vacancy concentration, which supported the explanation of strain localization behaviour better than hydrogen alone [49]. Thus, the fracture surface shows a highly localized plastic failure than brittle pattern. The researchers reported occurrence of HELP in wide variety of materials which have different crystal structures and proposed that this mechanism is able to predict in general the influence of hydrogen on deformation (both elastic and plastic) and fracture.

As Birnbaum et al. [48] discuss, it is clear that the flow stress in area of localization is reduced relatively to the flow stress in the homogeneously deforming volume, but the mechanism of hydrogen causing shear localization has not been established yet.

Hydrogen Enhanced Decohesion (HEDE)

Troiano suggested that dissolved hydrogen (lattice hydrogen) could reduce the strength of inter-atomic bonds i.e. cohesive strength of the lattice and hence promotes decohesion. Oriani further developed Troiano's concept and proposed a mechanistic theory of lattice de-cohesion by hydrogen. This mechanism is supported primarily by the observations that in some non-hydride forming materials, hydrogen embrittlement appears to occur in the absence of significant local deformation. Probably no direct experimental measurements are present

which can support this mechanism. McMahon and co-workers advanced the view that impurity element segregated to grain boundaries similarly reduced parent-metal bond cohesion, adding to the embrittling effect of hydrogen [50]. The HEDE provides the basic explanation that hydrogen damage happens in the crack tip fracture process zone when local crack tip opening tensile stress exceeds the maximum local atomic cohesion strength, retarded by the presence of hydrogen [51]. The stress concentrated in FPZ can also be induced by various types of hydrogen trapping sites (for example inclusions, micro voids and impurity elements segregated to grain boundaries). In the HEDE mechanism, hydrogen damage sites are located at a distance ahead of the crack tip surface where tensile stresses may be maximized. Some dislocation activity may accompany decohesion, and may locally enhance stresses at decohesion sites, but should be limited so that atomically sharp crack tips are not blunted. High concentrations of hydrogen and decohesion event could happen at a variety of locations.

Very high elastic stresses are probably required to generate sufficiently high concentrations of hydrogen in interstitial lattice sites ahead of crack tips to produce decohesion. Due to hydrogen trapped at specific sites, decohesion at grain boundaries could occur at or ahead of crack tips due to bond weakening by hydrogen. Since intergranular fracture mode has been observed in hydrogen degraded steels, especially in carbon steel with hydrogen segregating at grain boundaries, the HEDE seems to explain the grain boundary decohesion. In carbon steels and austenitic steels, cleavage fracture as well as quasi-cleavage and ductile fracture have been observed [45]. Each mechanism which is supposed to explain hydrogen effect on mechanical properties includes several factors acting simultaneously, which may not suitable for some specific materials or conditions. In the actual situation, different mechanisms may take place at the same time and interact with each other [48].

2.3 Factors influencing delayed fracture

Lattice defects

Delayed fracture in the structural steels are greatly influenced by lattice defects. The value of binding energies are different for different lattice defects and result in different hydrogen-lattice defect interactions. Bond et al. proposed the HELP theory which stated that hydrogen facilitates dislocation movement and promotes planar slip by stabilizing the edge component of dislocations. That is why, when hydrogen is present, the critical shearing stress for planar slip is more easily reached. When the obstacles such as solid inclusions or clusters of mechanical twins and rigid secondary phase, are present in the materials, they hinder the dislocation movement then crack embryos are ready to form. Since hydrogen has high affinity to the mentioned obstacles, hydrogen atoms accumulate around the obstacles and further reduce the critical stress for crack initiation. Kim et al. proposed that banded structure observed or micro-cracks formed near to inclusions in some hydrogen charged high strength steels. Depending on distribution and geometry, different types of obstacles affect DF behaviour in different manner. Generally, the inclusions or precipitates at the grain boundaries would most probably be detrimental to HIC. Thus, grain size refining, high grain boundary purity and avoiding high stress concentration at grain boundaries would be helpful in improving DF resistance.

Phase structure

In addition to the lattice defects, a wide range of phase structures also influenced the DF behaviour in structural steels. Generally, materials having BCC, the martensite or tempered martensite structure are more susceptible to delayed fracture because they have high sensitivity to hydrogen due to low solubility and high diffusivity of hydrogen. FCC structure is less susceptible to delayed fracture because it has high solubility and low diffusivity of hydrogen. Hence, FCC structure shows excellent resistance to delayed fracture.

Alloying elements

Hydrogen behaviour in steels is greatly influenced by different alloying elements. Elements such as Ni, Mn, Cr, Ti, Nb decrease hydrogen diffusivity and increase hydrogen solubility

whereas elements such as C, N, Al, Si, Co, Mo increase hydrogen diffusivity and decrease hydrogen solubility. In high manganese steel, Mn and C stabilize austenite and in these steels sulphur and phosphorus content should be kept low to prevent their segregation at grain boundaries or forming sulphides. Addition of Al in high manganese steel reduces delayed fracture but the mechanisms were not fully studied.

Strength

Generally it is believed that as the strength of steel increases, the susceptibility to HE also increases. High strength steels having ultimate tensile strength approximate 700 MPa, should not be used in hydrogen environments due to their threshold stresses, which are significantly less than those thresholds under benign conditions. Ultra-high strength steels having ultimate tensile strength approximate 1400 MPa, become extremely susceptible to HE [27]. Some other studies described that threshold stress intensity for crack initiation or crack growth increases with increasing yield strength.

Temperature

Hydrogen behaviour and deformation mechanism both influenced greatly by temperature. As the temperature increases from RT to 300^0C, hydrogen diffusivity also increases [52]. When the temperature is above 200^0C, most diffusive hydrogen comes out from the material. It helps to minimize the influences of internal diffusive hydrogen and inducing the recovery of mechanical properties from hydrogen embrittlement. When the hydrogen is present in low temperature formed component, hydrogen would be active with increasing temperature. Hydrogen diffuses to various lattice defects or crack tips and results in DF.

Strain Rate

Hydrogen damage is very sensitive to strain rate because hydrogen always takes some time to interact with dislocations. If the strain rate is high then hydrogen will not get any time to interact with dislocation movement, like in quasi-static tensile test. Also the adiabatic heating due to increased strain rate would probably discharge the diffusive hydrogen from the bulk material.

CHAPTER 3: PLAN OF WORK, MATERIALS INVESTIGATED AND PROPERTIES OF MATERIALS

3.1 Plan of work

In the current work, two types of specimens of each investigated materials were taken: tensile, notched tensile specimens and round blanks. First these were pre-charged by electrochemical hydrogen charging method. After charging tensile and notched tensile specimens were mechanically tested by slow strain rate test, to know hydrogen embrittlement effect. Pre-charged round blanks were drawn in cylindrical shape cups, to know delayed fracture phenomenon. After this SEM investigation of fracture surface was carried out.

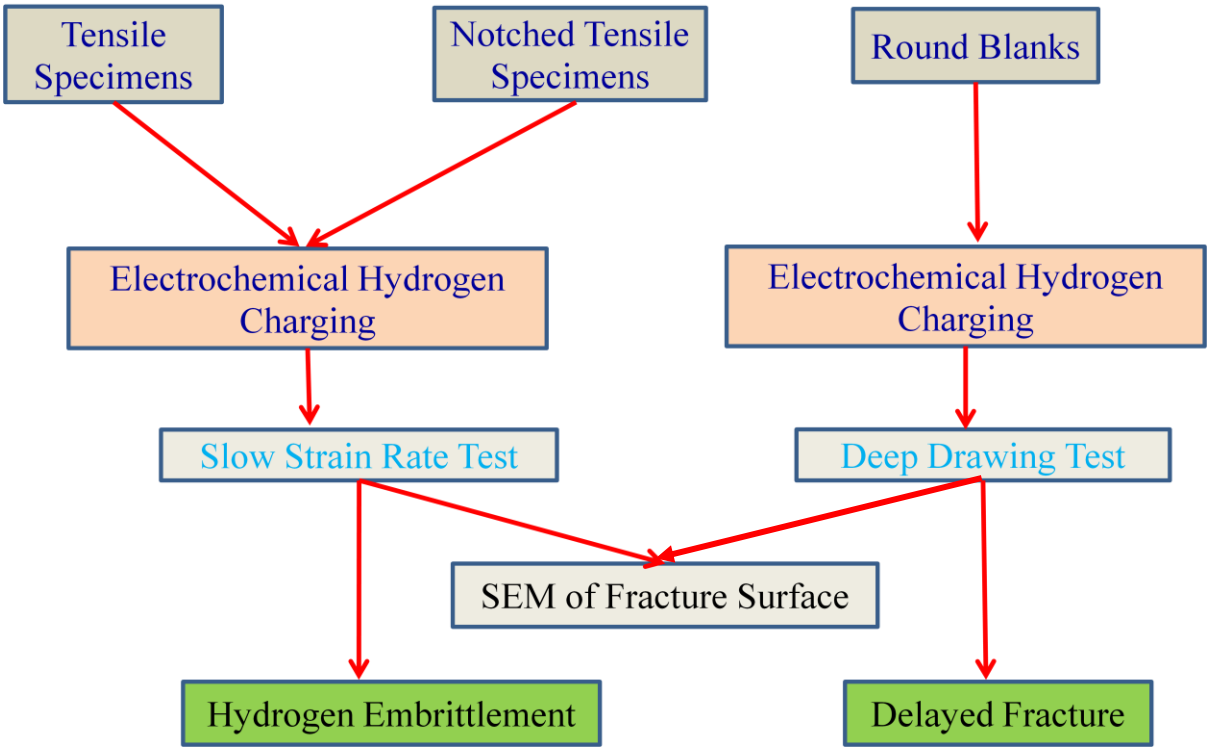

Figure 3.1: Schematic representation for the plan of work.

3.2 Materials Investigated

In this investigation four materials with different chemical compositions of alloying elements have been studied to clarify the influence of hydrogen on DF. Among four, two are high manganese TWIP steels with main differences in C and Al contents, and rest two are TRIP 800 and DP 780. TWIP steels are fully austenitic steels. TRIP is a combination of austenite, bainite and martensite structure whereas DP is combination of ferrite and martensite structure. Some parameters related to materials properties which influence DF behaviour are summarized as follows:

1) Influences of alloying elements: C, Mn, Al
2) Influences of deformation mechanisms: TWIP or TRIP
3) Influences of tensile strength: ranging from 700-1200 MPa.

The chemical compositions of the investigated materials are given in **Table 3.1.** Most of the materials were delivered in the cold-rolled and annealed condition.

Table 3.1: Chemical compositions of the investigated materials in mass %

Materials	C	Mn	P	S	Si	Cr	Ni	Al	Fe
X60Mn22	0.59	22.37	0.022	0.0014	0.24	0.074	0.03	0.0023	76.6
X30MnAl22-1	0.334	21.86	0.01	0.0033	0.046	0.032	0.038	1.3	76.3
TRIP 800	0.21	1.62	0.001	0.001	1.6	0.042	0.025	0.0036	96.4
DP 780	0.13	1.85	0.012	0.001	0.24	0.372	0.037	0.0035	97.3

3.3 Deformation mechanisms and the stability of austenite in Investigated steels

The deformation mechanisms in austenitic steels are greatly influenced by Stacking Fault Energy (SFE). Literature reviews concluded that transformation of austenite γ to cubic martensite ά through γ→ ά or γ→ ε →ά (ε-hexagonal martensite) will be the favourable deformation mechanism when the material has γ_{SFE} value below 18 mJ/m^2, the deformation is manifested by mechanical twinning when 18 mJ/m^2 < γ < 45 mJ/m^2, dislocation sliding

dominates when γ > 45 mJ/m^2 [53,55-56,57]. For high manganese austenitic steels, the calculated γ_{SFE} based on thermodynamic model according to Akabari [55] and empirical equation according to Dumay [56]. X60Mn22 and X30MnAl22-1 deformed through mechanical twinning (TWIP effect) and no ά- or ε-martensite has been found in them, which are also in accordance with other literatures [53,54,56].

3.4 Mechanical properties

Mechanical properties of the investigated materials were characterized in QTT. **Figure 3.2**, showed the engineering stress-strain curve identified by the QTT at the strain rate of 10^{-3}/s. The TWIP steels showed excellent ductility at high tensile strengths. All the austenitic steels achieved extraordinary high elongation values due to the postponed necking by phase transformation or mechanical twinning. X60Mn22 and X30MnAl22-1 exhibit superior strength and elongation combinations. In comparison, X60Mn22 has higher strength than X30MnAl22-1, which is supposed due to the early twinning and higher twinning intensity compared to X30MnAl22-1.

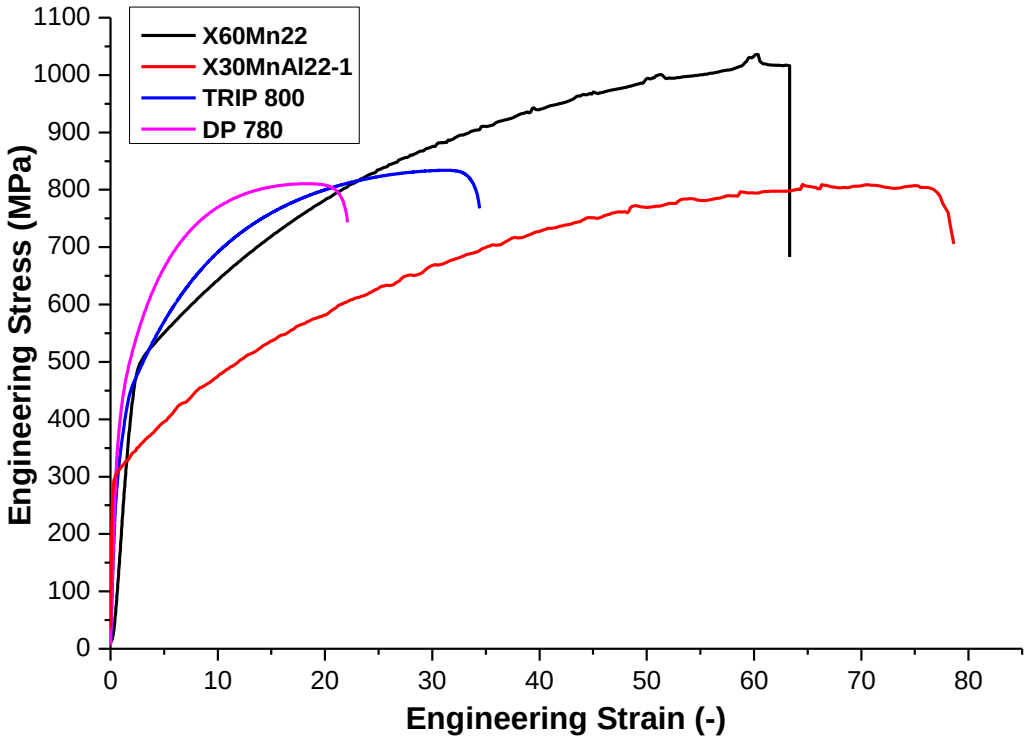

Figure 3.2: Engineering stress-strain curves of the investigated materials evaluated by quasi-static tensile test at the strain rate of 10^{-3}/s and room temperature.

CHAPTER 4: EXPERIMENTAL METHODS

4.1 Hydrogen charging

The as delivered materials contain a little amount of hydrogen (less than 3 ppm). Hydrogen can be further introduced by electrochemical charging. There are two charging methods to introduce hydrogen into materials:

1. Potentio-static charging
2. Galvano-static charging

A computer controlled potentiostat was used to perform potentio-static charging and galvano-static charging as shown in **Figure 4.1**. The set-up of potentio-static charging and galvano-static charging station are shown in **Figure 4.2.**

The potentio-static charging station consists of three-electrode. Calomel electrode worked as reference electrode and platinum net worked as the counter electrode. Specimen worked as the cathode. The solution of 0.05 M H_2SO_4 (sulphuric acid) and 1.4 g/l CH_4N_2S (thiourea) and voltage of -800 mV_{SCE} was applied.

The galvano-static charging station consists of two-electrode. Platinum net worked as anode and specimen worked as cathode. The solution of 0.05 M H_2SO_4 (sulphuric acid) with 1.4 g/l CH_4N_2S (thiourea) and the current density of 0.5 mA/cm^2 (168 hours), 2.5 mA/cm^2(24 hours), 5 mA/cm^2 (24 hours) was used to charge round blanks. CH_4N_2S (thiourea) act as poison agent which slow down the combination of H to hydrogen molecule, which promotes hydrogen entry effectively.

For SSRT, both tensile and notched tensile specimens were charged by potetio-static method but for DDT, specimens were charged by both potentio-static and galvano-static method. Charging solution 2 litres by volume was used in each charging procedure. Mechanical stirring was used to homogenize the solution and eliminate polarization. In case of electrochemical charging in sulfuric acid electrolytes, the maximum charging temperature was limited to approximate 60 °C, above which the solution may evaporate quickly during charging. In this work, the charging solution was kept at room temperature for both type of

charging. Nitrogen gas was supplied for approximate half an hour into the solution to take away dissolved oxygen gas which promotes oxidation and prevents hydrogen entry.

Before charging, the specimen surfaces were polished with 320, 500, 800, 1200- grit emery paper then fine polished with 6µ and 1µ grit paper, followed by cleaning in ethanol and drying. The surfaces which need to be charged, were exposed to charging solution and other parts were covered with Teflon band. The specimens for different charging purposes are shown in **Figure 4.3**. In potentio-static charging there is no rusty layer on specimen surface. After galvano-static charging there is rusty layer created on specimen surface which was removed with 1200-grit emery paper for measurement accuracy. After charging, the specimens were cleaned and stored in liquid nitrogen (-196 °C) to prevent hydrogen loss until mechanical testing.

Diffusivity of hydrogen is slow in austenitic steels, fully homogeneous distribution of hydrogen needs several months charging under laboratory condition. In this study, the specimens were charged for 24,72 hours and 168 hours to do some mechanical testing.

Figure 4.1: Computer controlled potentiostat.

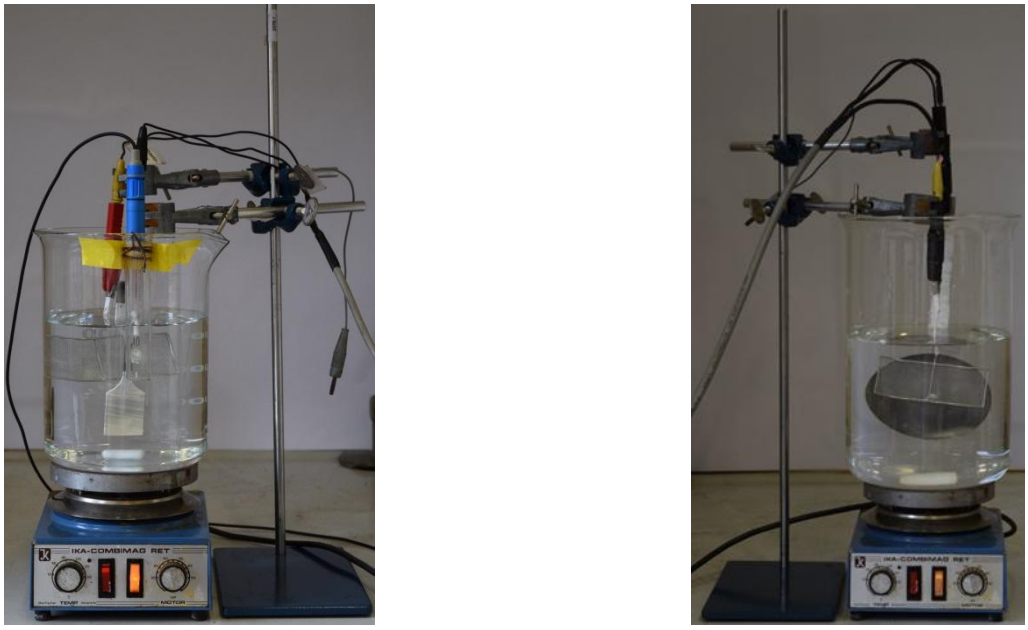

(i) (ii)

Figure 4.2: (i) Potentio-static hydrogen charging station (ii) Galvano-static hydrogen charging station.

(i) (ii)

Figure 4.3: (i) DDT specimen for hydrogen charging (ii) Tensile and notched tensile specimen for hydrogen charging.

4.2 Mechanical Tests

4.2.1 Quasi-static Tensile Test (QTT)

Quasi-static tensile test (QTT) was performed by a universal testing machine Zwick Z100/TL3S. Standard specimens with gauge length of 80 mm were used to perform QTT. Specimens were tensile deformed at room temperature with constant strain rate of 10^{-3}/s. After that Engineering stress-strain curve were plotted to know the value of stress and strain of the investigated materials in uncharged condition.

4.2.2 Slow Strain Rate Test (SSRT)

Constant extension machine (FRITZ Company) with a maximum load of 30 kN is used for slow strain rate test (SSRT), as shown in **Figure 4.4**. It is well known that SSRT technique provides information about hydrogen embrittlement of the material when it is exposed to hydrogen rich environment. Due to this reason, SSRT has been used for the investigation of hydrogen embrittlement. An axial load sensor with measurement error less than 1% was used to measure loading force. The cross head speed was set to $2.5\times10^{-5}\ mm$/s, which results in the strain rate of 10^{-6}/s with the used geometry of specimen. The tensile specimen with gauge length of 25 mm and width of 5 mm and notched tensile specimen with gauge length of 25 mm, notch radius 0.125 mm, angle 45 degree, distance between notch 2.75 mm were pre-charged with hydrogen and tensile deformed at constant strain rate of 10^{-6}/s. This strain rate is very slow for transporting hydrogen by moving dislocations under the driven force of stress gradient. V-notch is created in tensile specimen to know the effect of complex stress state under the influence of hydrogen. The specimens were pre-charged with different amounts of hydrogen. The tensile load and displacement were recorded every 5 minutes till fracture, which were converted into stress-strain curves and force-displacement curves. By SSRT we get the data to compare the parameters (maximum stress, strain, time to failure etc.) obtained with different hydrogen content. Mechanical properties such as yield strength (YS), tensile strength (TS), uniform elongation (UE), total elongation (TE) and flow curves are determined by SSRT, which can reveal the effects of hydrogen contents on mechanical properties. During SSRT, oversaturated hydrogen atoms diffuse to crystal defects and recombine to hydrogen molecules, which creates a large internal pressure that increases micro void growth and crack initiation. Hydrogen atoms diffuse due to stress gradient and

accumulate ahead of crack tips, weakening bond cohesion force in materials. The absorption of hydrogen adjacent to a crack decreases the surface free energy of the material and decreases the energy needed for fracture, which increases crack propagation.

The load value and time to fracture were measured by software scanscape. Stress loss and strain loss can be calculated by the following equations:

$$stress\ loss(\%) = \frac{(\sigma_{uncharged} - \sigma_{H\ charged})}{\sigma_{uncharged}} \times 100\% \quad (4\text{-}1)$$

$$strain\ loss(\%) = \frac{(\varepsilon_{uncharged} - \varepsilon_{H\ charged})}{\varepsilon_{uncharged}} \times 100\% \quad (4\text{-}2)$$

After calculating values by these equations it was cleared that there are percentage loss in strain in the hydrogen pre-charged specimens compared to uncharged specimens. In ductile failure, during elastic-plastic deformation voids are generated within the necked region of the tensile specimens and coalescence of voids occurred to create an internal crack by normal fracture. Final fracture took place by shear rupture. Creation of voids in ductile fracture surface can be seen in the form of dimples in the microstructure.

Figure 4.4: The constant extension machine with maximum load of 30 kN for performing slow strain rate test.

When hydrogen charged steel specimens loaded in SSRT machine show failure by brittle fracture with no necking and absence of cup and cone fracture surface. Brittle failures are characterized by rapid crack propagation with less energy consumption than ductile failure. Brittle fracture has a bright granular appearance and shows little or no necking. The fracture surface of steel specimens also show the presence of shear slip along the periphery where crack generates from inner part of surface.

High manganese TWIP steels and other AHSS possess high strength and good ductility. SSRT provide useful information about behaviour of High manganese TWIP steel and other AHSS under charged and uncharged conditions. After hydrogen charging, a significant drop in % elongation is observed which lead to hydrogen embrittlement effect and failure mode appears to be brittle on fracture.

4.2.3 Deep Drawing Test (DDT)

Deep Drawing Test (DDT) is used to investigate the delayed fracture behaviour of the materials. DDT is performed by ERICHSEN 142/40 sheet testing machine. ERICHSEN 142/40 sheet testing machine for deep drawing test is shown in **Figure 4.5.** DDT is a widely used sheet metal forming process. The round blank specimens were drawn into cylindrical shape cup through the lifting motion of a punch. The edge of the blank should be neatly polished to avoid the crack caused by rough surface. DDT is also a basic mechanical test for sheet metal formability. Plastic film and oil are used as lubricant in order to reduce the effect of friction. The blank holder force (BHF) in kN, punch velocity (PV) in mm/min, drawing ratio (DR=$\Phi_{specimen}/\Phi_{punch}$), forming rate and temperature are important parameters in DDT and controlled by machine set up. Residual stress with high triaxiality is induced in DDT.

The part of blank which comes in contact with front of punch, will form bottom of the cup. It shows the minimum variation in thickness. The part of blank which will form the sidewall of the cup and the flange, has undergone bending around the die radius and then unbending as it is drawn to become the side wall.

After the deep drawing process, a residual stress state will remain in the deep drawn cup, which could also be an important influencing factor of delayed fracture. In order to

investigate hydrogen induced delayed fracture, comparison experiments are operated. Specimens with and without hydrogen charging are tested under the same experiment parameters.

Figure 4.5: ERICHSEN 142/40 sheet testing machine for deep drawing test.

4.3 Scanning Electron Microscope (SEM)

ZEISS DSM 982 Scanning Electron Microscope was used to investigate the morphology of the fracture surfaces of specimens at an operating voltage of 15kV. It is a kind of electron microscope that images a sample by scanning it with a beam of electrons in a raster scan pattern. The electrons interact with the atoms and produce signals that contain information about the sample's surface topography, composition and other properties such as electrical conductivity. The set up is shown in **Figure 4.6.**

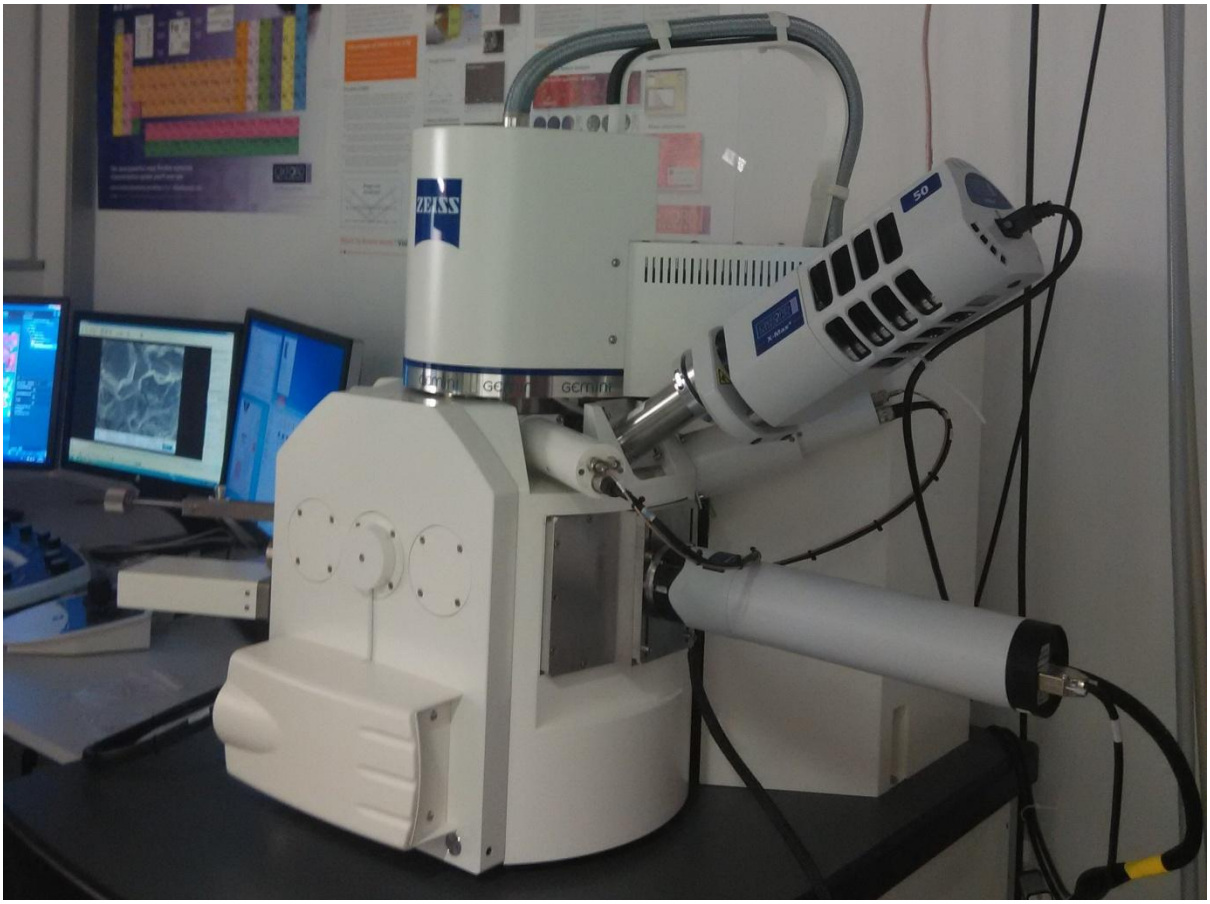

Figure 4.6: Set up of scanning electron microscope (SEM).

CHAPTER 5: RESULTS

This chapter deals with the results related to hydrogen effect on mechanical properties and fracture behaviour of the investigated materials after Slow Strain Rate Test (SSRT) and Deep Drawing Test (DDT).

The effects of hydrogen on mechanical properties were characterized quantitatively and correlated to the respective alloying concept and phase stability. The fracture surfaces of both hydrogen pre-charged and uncharged specimens were investigated under Scanning Electron Microscopy (SEM).

Different mechanical tests provided information about the influence of hydrogen on the DF of various steels. Slow strain rest test (SSRT) were employed on both tensile and notched tensile specimens to evaluate the effects of diffusible hydrogen on the hydrogen embrittlement properties of steels. Deep drawing test (DDT) was conducted to evaluate the effect of stress state on DF behaviour of steels.

5.1 Outcome of slow strain rate test (SSRT)

5.1.1 Mechanical Properties of uncharged and hydrogen charged tensile specimens

The Engineering stress-strain curve for the investigated materials (uncharged specimens and hydrogen pre-charged specimens) obtained are shown in **Figure 5.1.** Significant reductions in strain with increasing charging hours were observed in all the investigated materials i.e. strain losses were obviously affected by increasing hydrogen charging hours from 72 to 168 hours. However negligible changes in work-hardening behaviour were observed between hydrogen pre-charged and uncharged TWIP steels, TRIP and DP i.e. there is no significant change in the deformation behaviour after hydrogen charging. Hydrogen pre-charged specimens did not show any necking before fracture but showed the quick reduction in load after the peak load. The same behaviour was observed in uncharged specimens of X60Mn22, X30MnAl22-1 which have some amount of hydrogen initially (between 1 to 3 ppm). The absence of the necking phenomenon after uniform deformation shows the brittle transition of fracture behaviour due to the increased hydrogen content.

It is clear from the **Figure 5.1** that after 72 hours hydrogen charging, X60Mn22 and X30MnAl22-1 have almost same ductility loss but TRIP 800 and DP 780 have higher ductility loss as compared to both TWIP steels. But as the charging hours were increased upto 168 hours, X60Mn22 showed higher ductility loss as compared to X30MnAl22-1. Hence, X30MnAl22-1 is less susceptible to hydrogen embrittlement (HE) as compared to X60Mn22. After 168 hours of charging, TRIP 800 and DP 780 showed very high ductility loss as compared to both TWIP steels. As a result it can be concluded that TRIP 800 and DP 780 are more prone to HE as compared to both TWIP steels. If comparison is made only between TRIP 800 and DP 780 then DP 780 showed larger ductility loss as compared to TRIP 800 after hydrogen charging so it can be concluded that DP 780 is more susceptible to HE as compared to TRIP 800.

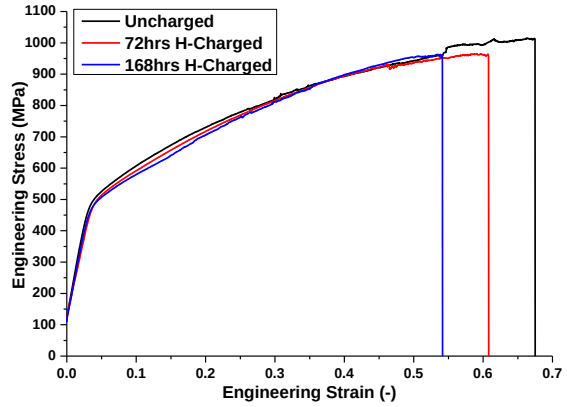

a) X60Mn22

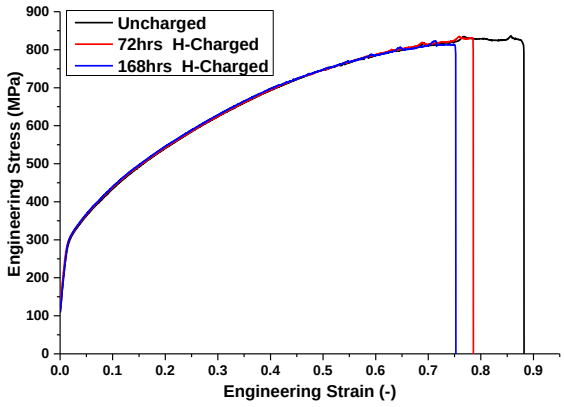

b) X30MnAl22-1

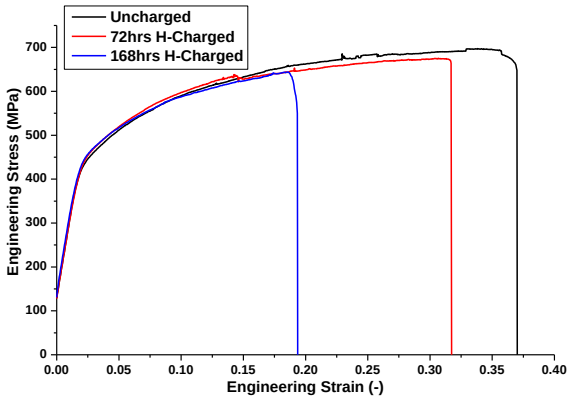

c) TRIP 800

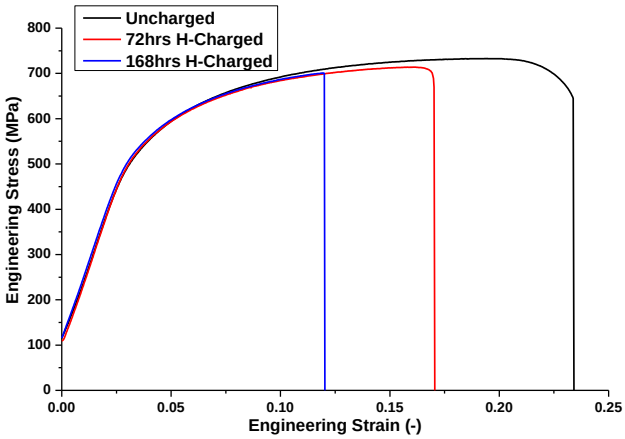

d) DP 780

Figure 5.1: Engineering stress-strain curve for uncharged and hydrogen pre-charged SSRT tensile specimens at constant strain rate of 10^{-6}/s: a) X60Mn22, b) X30MnAl22-1, c) TRIP 800, d) DP 780

According to **equation (4-1)** and **(4-2),** stress and strain losses were calculated by taking average values of stress and strain after getting from three experiments at each charging condition, applied some statistics and plotted in **Figure 5.2.**

It is clear from **Figure 5.2** that as the hydrogen charging hours increased, stress and strain losses for all the investigated materials also increased, but it can be clearly seen that hydrogen has severe effect on ductility as compared to tensile strength.

The strain losses in TRIP 800 and DP 780 reached more than 40% with 168 hours of hydrogen charging. The strain losses in high manganese TWIP steels (X60Mn22 and X30MnAl22-1) found lesser as compared to TRIP 800 and DP 780 steel.

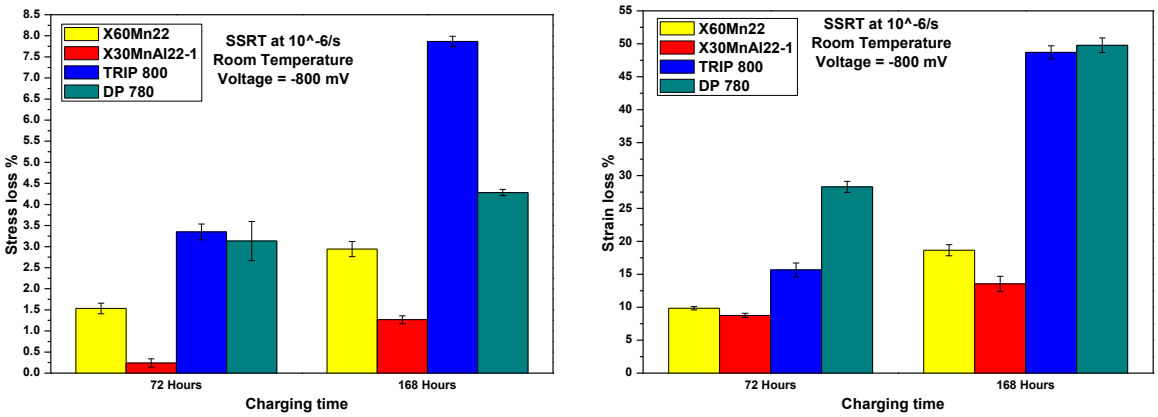

Figure 5.2: The embrittlement indexes of stress and strain losses with increasing hydrogen charging hours after SSRT at constant strain rate of 10^{-6}/s and room temperature for the investigated materials.

The strain losses for all the investigated materials were calculated from the values of strain which got from Figure 5.1 and shown in **Figure 5.3.**

It is clear from the **Figure 5.3** that upto 72 hours hydrogen charging, both TWIP steels have almost same value of strain loss but TRIP 800 and DP 780 have higher value of strain losses as compared to both TWIP steels. But as the charging hours were increased upto 168 hours, X60Mn22 showed increase in value of strain loss as compared to X30MnAl22-1. Hence, X60Mn22 is more prone to hydrogen embrittlement (HE) as compared to X30MnAl22-1. After 168 hours of charging, TRIP 800 and DP 780 showed very much increase in value of strain loss as compared to both TWIP steels. As a result it can be concluded that TRIP 800 and DP 780 are more susceptible to HE as compared to both TWIP steels. If comparison is

made only between TRIP 800 and DP 780 then DP 780 showed larger strain loss as compared to TRIP 800 after hydrogen charging so it can be concluded that DP 780 is more prone to HE as compared to TRIP 800.

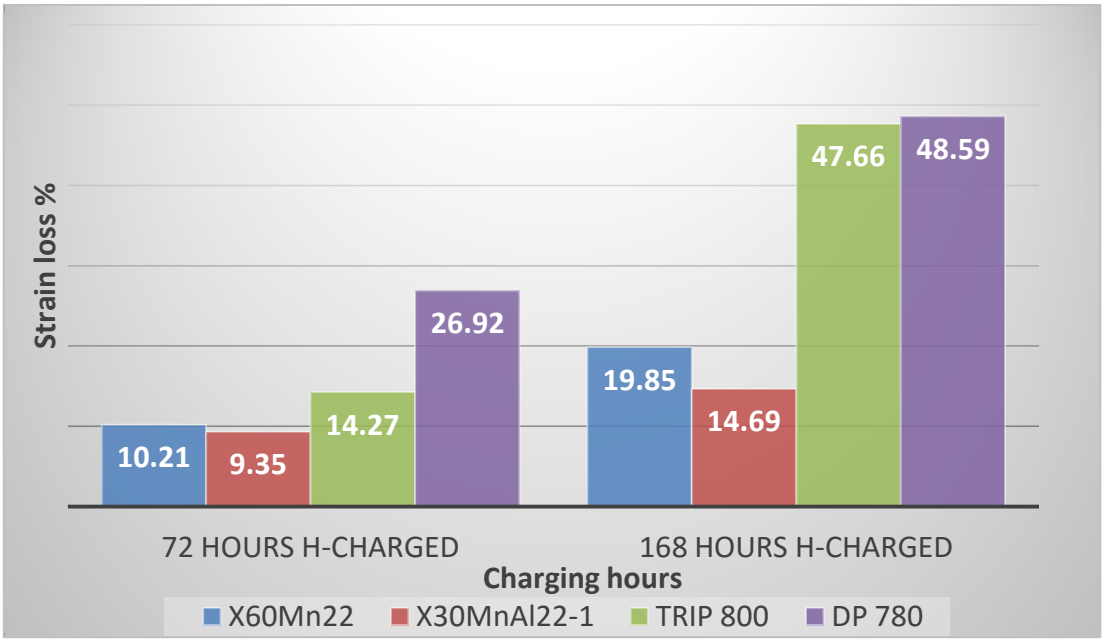

Figure 5.3: The strain loss % for the investigated materials with increasing hydrogen charging hours after SSRT at strain rate of 10^{-6}/s.

5.1.2 Fracture surface analysis of tensile specimens by SEM

The fracture surfaces of SSRT specimens (uncharged and hydrogen pre-charged) were analyzed by SEM. Fracture surface of hydrogen pre-charged specimens showed three different fracture zones: surface, sub-surface and middle, as sketched in **Figure 5.4**. For the uncharged specimens all three zones showed ductile fracture mode. The surface showed distinct brittle fracture mode due to severe hydrogen pre-charging. All the investigated materials showed the brittle fracture region in the surface, although the size of surface zone is different for different materials.

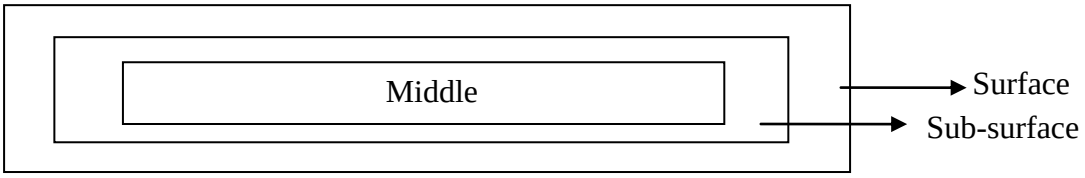

Figure 5.4: The surface, sub-surface and middle zone on the fracture surface of SSRT specimens.

In hydrogen charged specimens, the effect of hydrogen on the fracture mode in the sub-surface became prominent, indicating that the slow strain rate gave time for hydrogen interaction with dislocations and hydrogen redistribution. **Figure 5.5,** showed the SEM images of fracture surfaces of the investigated materials in uncharged and 168 hours hydrogen charged condition after SSRT.

For all the investigated materials in uncharged condition, fracture surfaces revealed overall ductile fracture behaviour throughout. As shown in Figure 5.5 a), the fracture surface of X60Mn22 in 168 hours hydrogen charged condition showed quasi-cleavage and intergranular brittle fracture mode in the surface zone. The sub-surface of 168 hours hydrogen charged specimen showed mixed ductile-brittle fracture mode and middle zone of fracture surface is still ductile after 168 hours of hydrogen charging. Since X60Mn22 has coarser grain size (low grain boundary area) and higher twin intensity, the observed fracture mode may result from the local accumulation of hydrogen at grain boundary or twins/grain boundary intersections. It provided substantial crack initiation sites and resulted grain boundary decohesion.

Figure 5.5 b) revealed the fracture surface of X30MnAl22-1 in 168 hours hydrogen charged condition. Quasi-cleavage fracture was observed only in the surface zone but the depth of quasi-cleavage fracture in X30MnAl22-1 is less as compared to X60Mn22 and fine dimples were observed in the sub-surface. Middle zone of fracture surface is completely ductile in nature. Clusters of AlN inclusions were also observed along with the dimples. X30MnAl22-1 has high fracture strength even after hydrogen pre-charging, but it exhibited low cleanness due to inclusions.

Figure 5.5 c) showed the fracture surface of TRIP 800 in 168 hours hydrogen charged condition. Quasi-cleavage fracture mode was observed in the surface zone. Some brittle facets were observed in the sub-surface and also below the sub-surface, which were assumed because retained austenite transformed into martensite phase. Martensite band appeared at some places in the fracture surface.

The fracture surface of DP 780 in 168 hours hydrogen charged condition showed quasi-cleavage fracture with some micro-cracks in the surface zone, as shown in Figure 5.5 d). Substantial brittle facets were also observed in the sub-surface. A large crack appeared in middle of fracture surface that is happen because of necking at the time of deformation and fast diffusion of hydrogen in ferrite and martensite phase.

Uncharged **168h H-Charged**

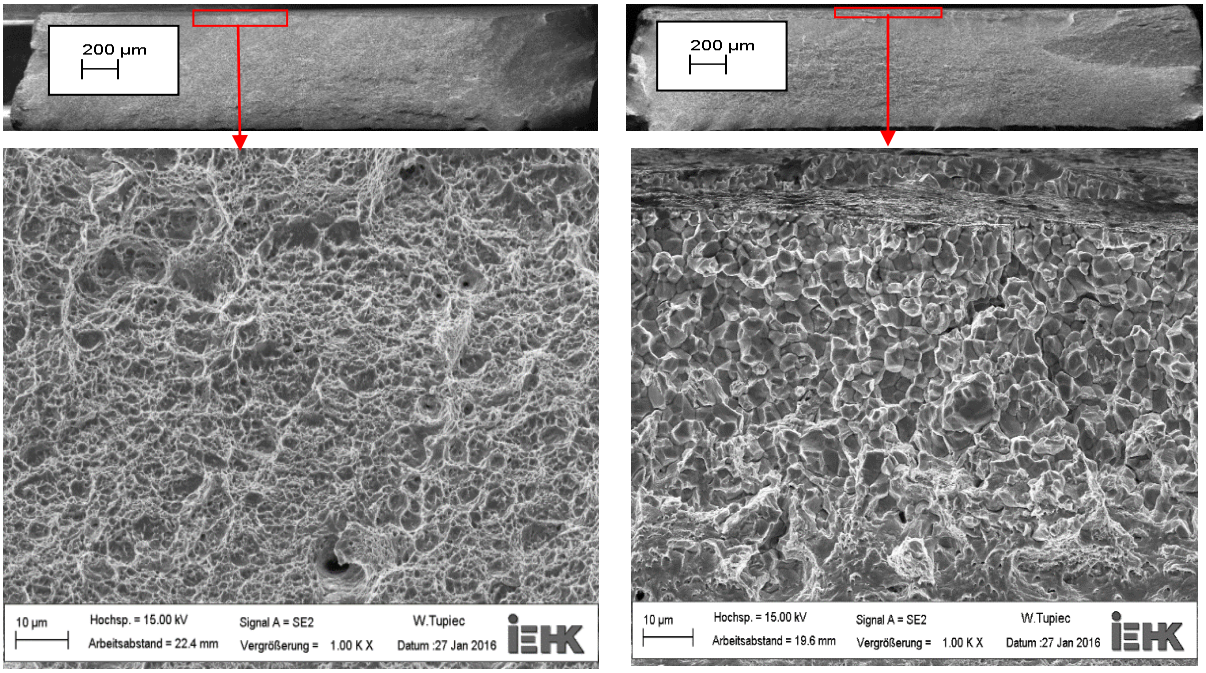

a) X60Mn22

Uncharged **168h H-Charged**

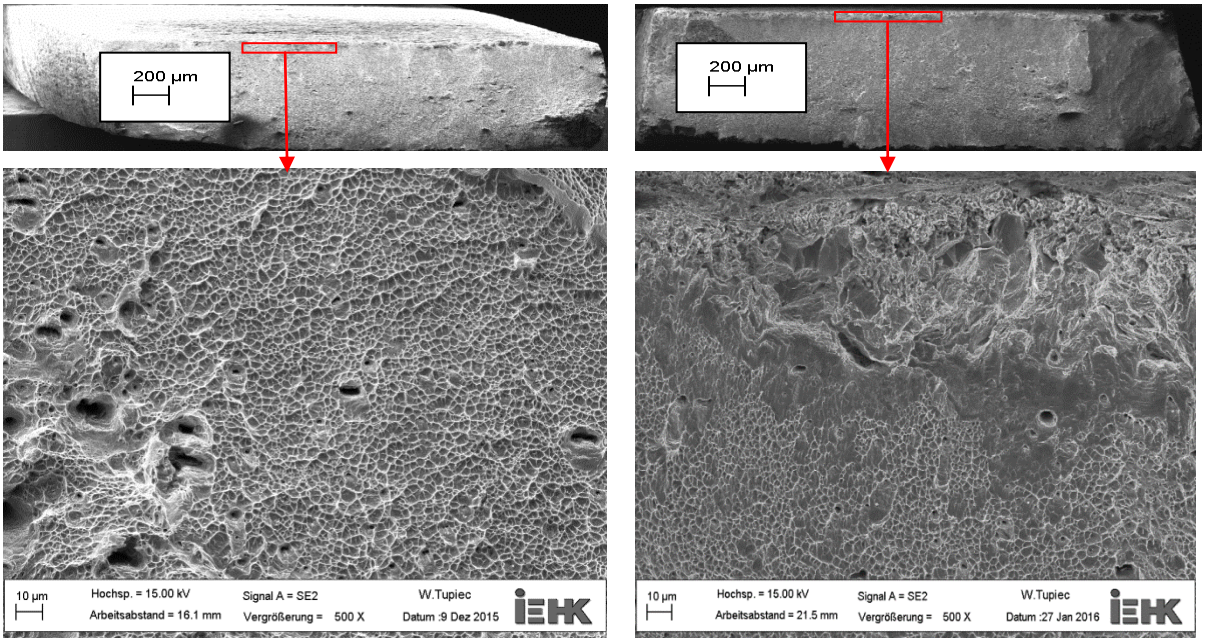

b) X30MnAl22-1

Uncharged **168h H-Charged**

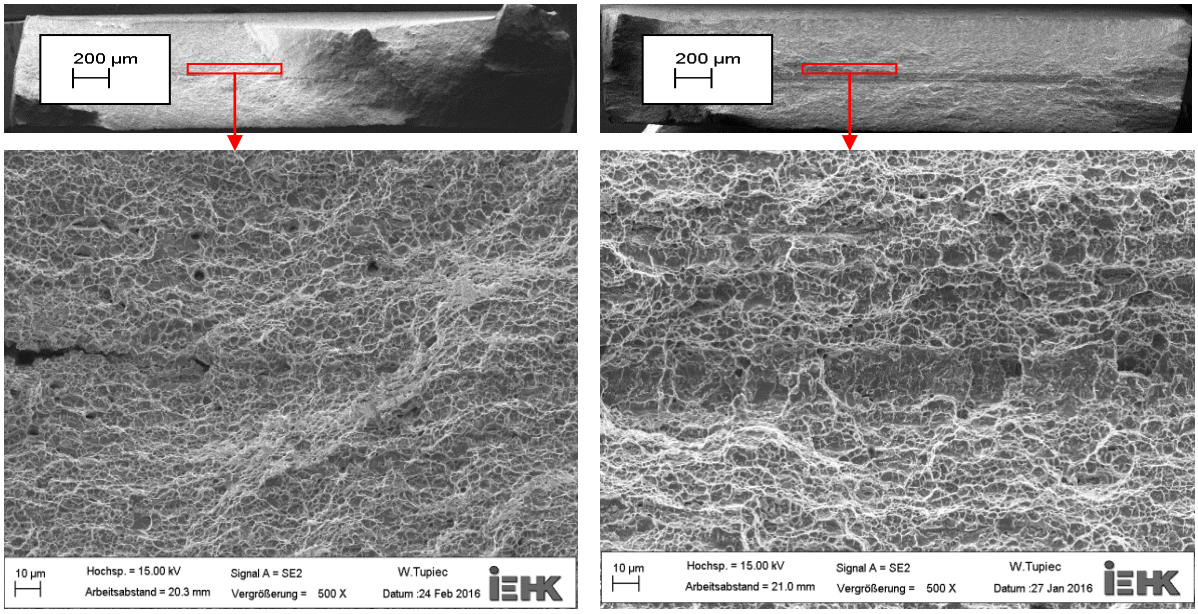

c) TRIP 800

Uncharged **168h H-Charged**

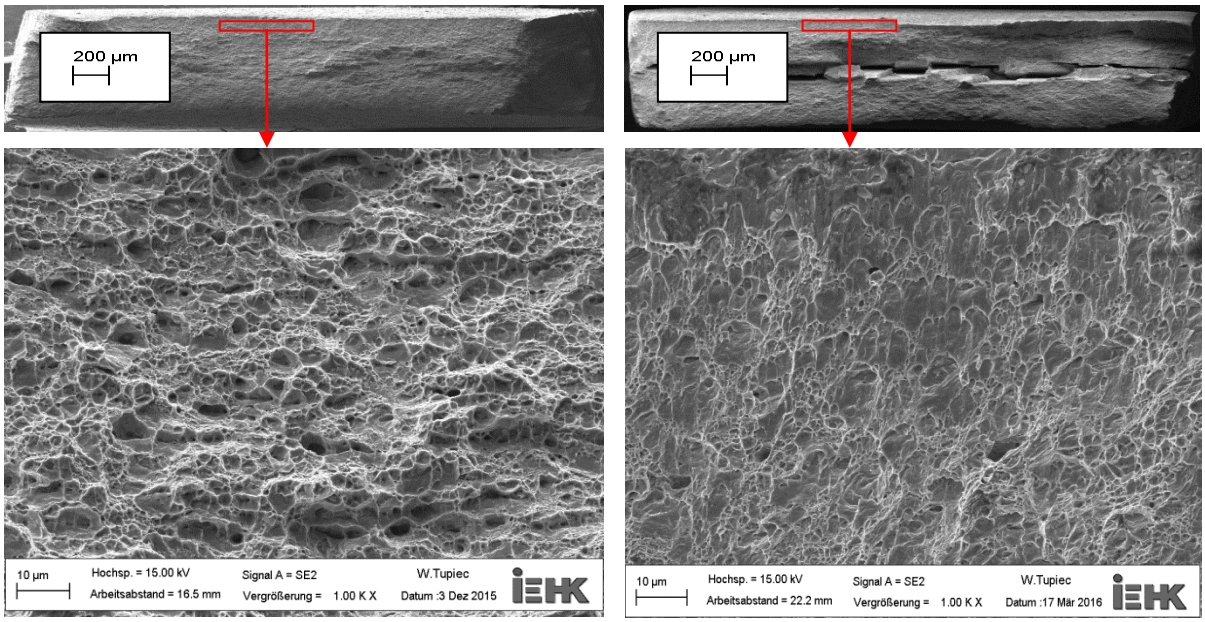

d) DP 780

Figure 5.5: SEM of the fracture surfaces of the investigated materials in uncharged and 168 hours of hydrogen charged condition after slow strain rate test.

5.1.3 Mechanical Properties of uncharged and hydrogen charged notched tensile specimens

The Engineering stress-strain curve for the investigated materials (uncharged specimens and hydrogen pre-charged specimens) obtained are shown in **Figure 5.6.** It is clear from the Figure that under complex stress state, with presence of hydrogen failure takes place much earlier due to crack initiation at the notch. The influence of complex stress state in notched tensile specimens was evaluated based on the reduction in strain for each material after hydrogen charging under the same environment.

The fracture process in the notched tensile specimen due to the presence of hydrogen can be considered as follows: 1) Hydrogen accumulated at the notch root and initiate crack due to the slip or the grain boundary crack occurs near to the notch root. 2) The hydrogen is concentrated at the nucleated crack, thus crack can propagate. The crack nucleated from one point or some points and propagates macroscopically in one direction. 3) The unstable final fracture is occured by the macroscopic shear stress.

It is assumed that the tensile strength degradation due to presence of hydrogen is caused by the faster crack nucleation and crack propagation due to hydrogen.

From **Figure 5.6,** it is clear that under complex stress state due to presence of hydrogen, all the investigated material showed reduction in strain but the extent of reduction is different for all the materials. X60Mn22 showed much faster crack initiation and propagation at notch as compared to X30MnAl22-1 because the difference in the strain between uncharged and hydrogen charged specimens for X60Mn22 is more as compared to X30MnAl22-1. Hence X60Mn22 is more influenced by complex stress state than X30MnAl22-1 under same experimental condition.

DP 780 showed much faster crack initiation and propagation at notch than TRIP 800 in complex stress state due to presence of hydrogen because the difference in the strain between uncharged and hydrogen charged specimens for DP 780 is more as compared to TRIP 800. So, DP 780 is more influenced by complex stress state than TRIP 800 under same experimental condition.

It is also clear that TRIP 800 and DP 780 steel have higher tendency to initiate crack at the notch than TWIP steels (X60Mn22 and X30MnAl22-1) due to presence of hydrogen under complex stress condition. Therefore, TRIP 800 and DP 780 steel are more influenced by complex stress state than TWIP steels under the same experimental condition.

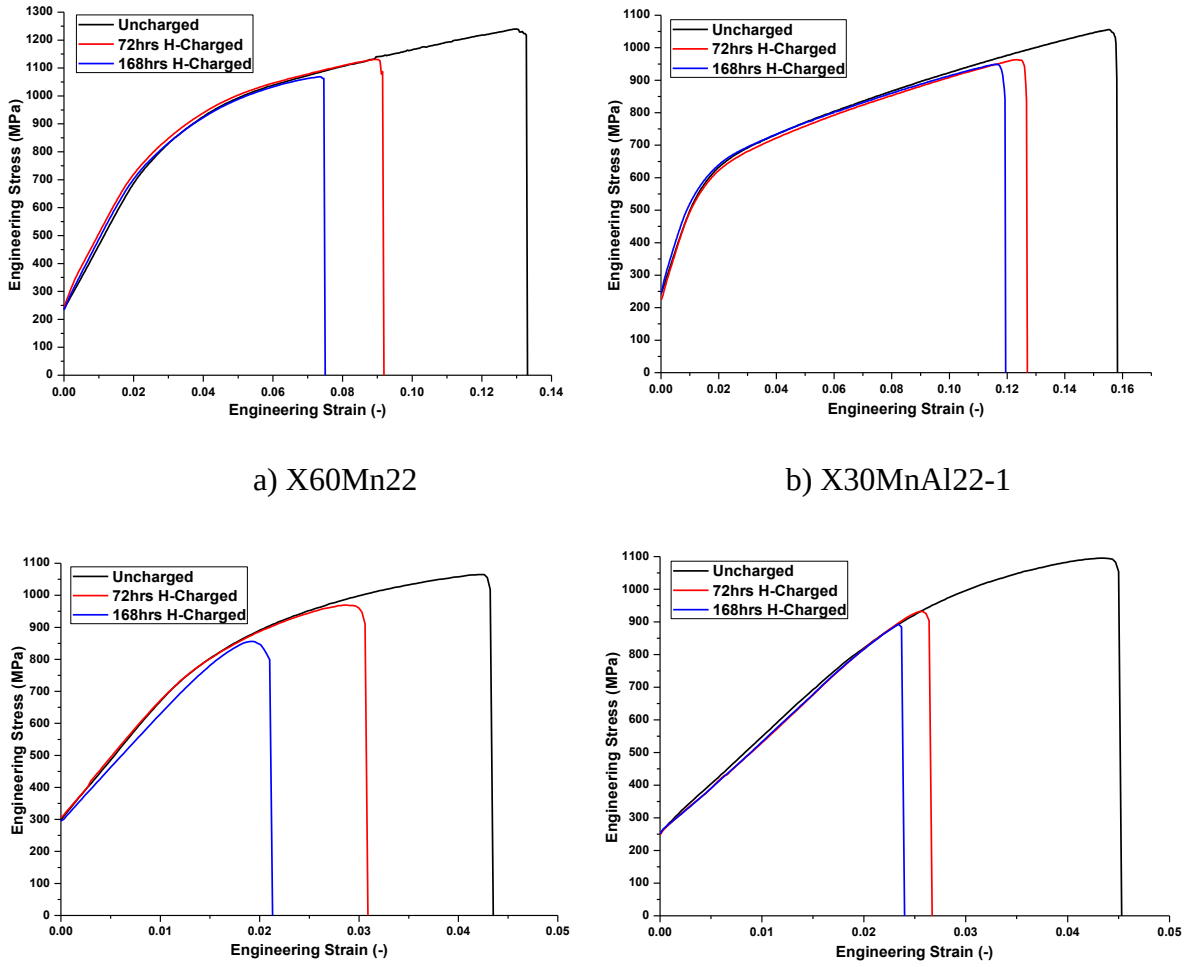

a) X60Mn22 b) X30MnAl22-1

c) TRIP 800 d) DP 780

Figure 5.6: Engineering stress-strain curve for uncharged and hydrogen pre-charged SSRT notched tensile specimens at constant strain rate of 10^{-6}/s: a) X60Mn22, b) X30MnAl22-1, c) TRIP 800, d) DP 780

According to **equation (4-1)** and **(4-2),** stress and strain losses were calculated by taking average values of stress and strain after getting from three experiments at each charging condition, applied some statistics and plotted in **Figure 5.7.**

It is clear from **Figure 5.7** that as the hydrogen charging hours increased, stress and strain losses for all the investigated materials also increased, but it can be clearly seen that hydrogen has severe effect on strain as compared to stress.

The stress and strain losses in TRIP 800 and DP 780 reached more than 15% and 40% respectively with 168 hours of hydrogen charging. The stress and strain losses in high manganese TWIP steels (X60Mn22 and X30MnAl22-1) found lesser as compared to TRIP 800 and DP 780 steel. Hence, under complex stress state with presence of hydrogen failure takes place much earlier in TRIP 800 and DP 780 steel as compared to high manganese TWIP steels (X60Mn22 and X30MnAl22-1) due to crack initiation at the notch.

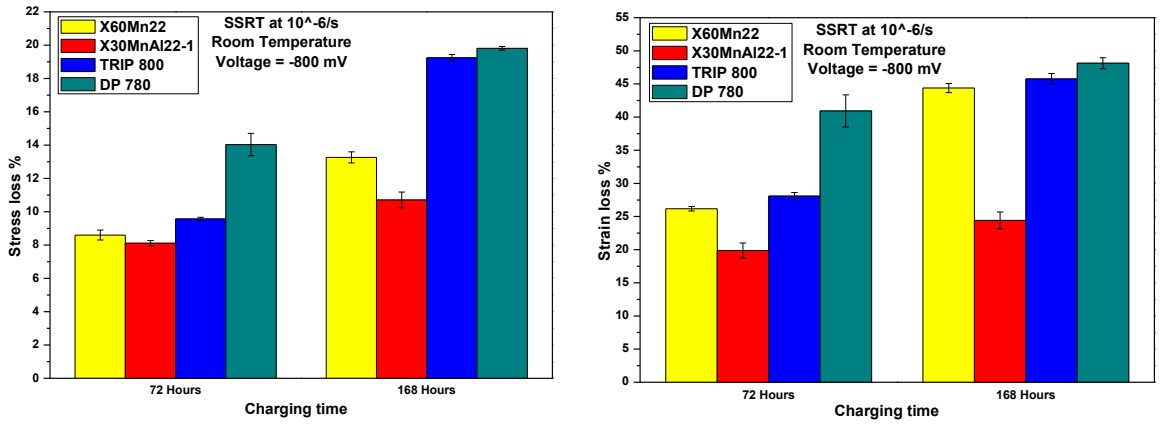

Figure 5.7: The stress and strain losses with increasing hydrogen charging hours after SSRT at constant strain rate of 10^{-6}/s and room temperature for the investigated materials.

The strain losses for all the investigated materials were calculated from the values of strain which got from Figure 5.6 and shown in **Figure 5.8.**

It is clear from the **Figure 5.8** that for 72 hours and 168 hours of hydrogen charging, X60Mn22 showed higher value of strain loss as compared to X30MnAl22-1. Hence X60Mn22 is more influenced by complex stress state than X30MnAl22-1 under same experimental condition.

For 72 hours and 168 hours of hydrogen charging, DP 780 showed high value of strain loss as compared to TRIP 800. Therefore, DP 780 is more influenced by complex stress state than TRIP 800 under same experimental condition.

If strain loss is compared among TWIP, TRIP and DP steels then it is clear that strain losses of TRIP 800 and DP 780 are higher as compared to both TWIP steels (X60Mn22 and X30MnAl22-1). Hence, it can be concluded that TRIP 800 and DP 780 are more influenced by complex stress state as compared to both TWIP steels for 72 hours and 168 hours of hydrogen charging.

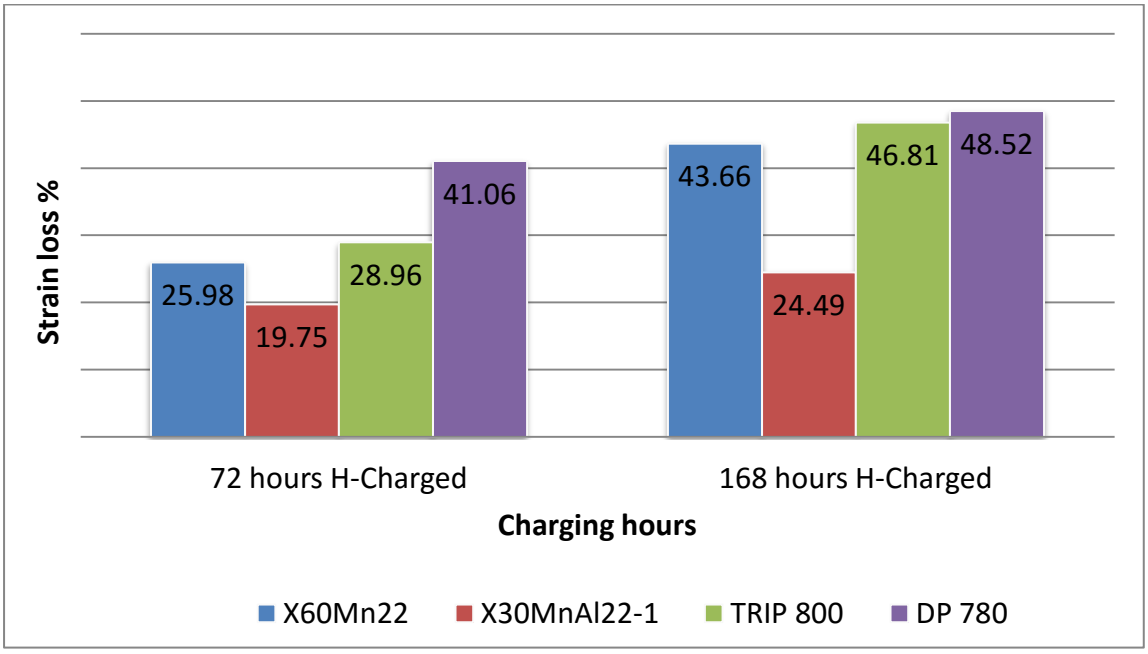

Figure 5.8: The strain loss % for the investigated materials with increasing hydrogen charging hours after SSRT at strain rate of 10^{-6}/s.

5.1.4 Fracture surface analysis of tensile specimens by SEM

Figure 5.9, showed the SEM images of fracture surfaces of the investigated materials in uncharged and 168 hours hydrogen charged condition after SSRT.

For all the investigated materials in uncharged condition, fracture surfaces revealed overall ductile fracture behaviour throughout (near to the notch and away from the notch). The unstable final fracture is occured by the macroscopic shear stress. The macroscopic shear fracture path was observed in most of the fracture surfaces. The intergranular fracture surfaces increase and the dimple fracture surfaces decrease with increasing hydrogen charging hours.

As shown in Figure 5.9 a), the fracture surface of X60Mn22 in 168 hours hydrogen charged condition showed quasi-cleavage and intergranular brittle fracture mode near to the notch. The surface which is little far away from notch of 168 hours hydrogen charged specimen showed mixed ductile-brittle fracture mode.

Figure 5.9 b) revealed the fracture surface of X30MnAl22-1 in 168 hours hydrogen charged condition. Intergranular fracture was observed only near to the notch but the depth of intergranular fracture near to notch in X30MnAl22-1 is less as compared to X60Mn22 and dimples were observed at little far away from notch. Clusters of AlN inclusions were also observed along with the dimples. X30MnAl22-1 has high fracture strength even after hydrogen pre-charging, but it exhibited low cleanness due to inclusions.

As shown in Figure 5.9 c), the fracture surface of TRIP 800 in 168 hours hydrogen charged condition exhibited quasi-cleavage fracture mode close to the notch. A large crack initiated near to the notch and smaller secondary micro cracks were present close to the large crack as well as in the region ahead of it. It was clearly stated in previous work [67] that the generated small cracks are hydrogen induced. Some brittle facets were observed at some distance from notch, which were assumed because retained austenite transformed into martensite phase. Martensite band also appeared at some places in the fracture surface.

As shown in Figure 5.9 d), the fracture surface of DP 780 in 168 hours hydrogen charged condition showed quasi-cleavage fracture with some micro-cracks near to the notch.

Substantial brittle facets were also observed at some distance away from notch. A large crack appeared in middle of fracture surface at some distance from notch that is happen because of fast diffusion of hydrogen in ferrite and martensite phase.

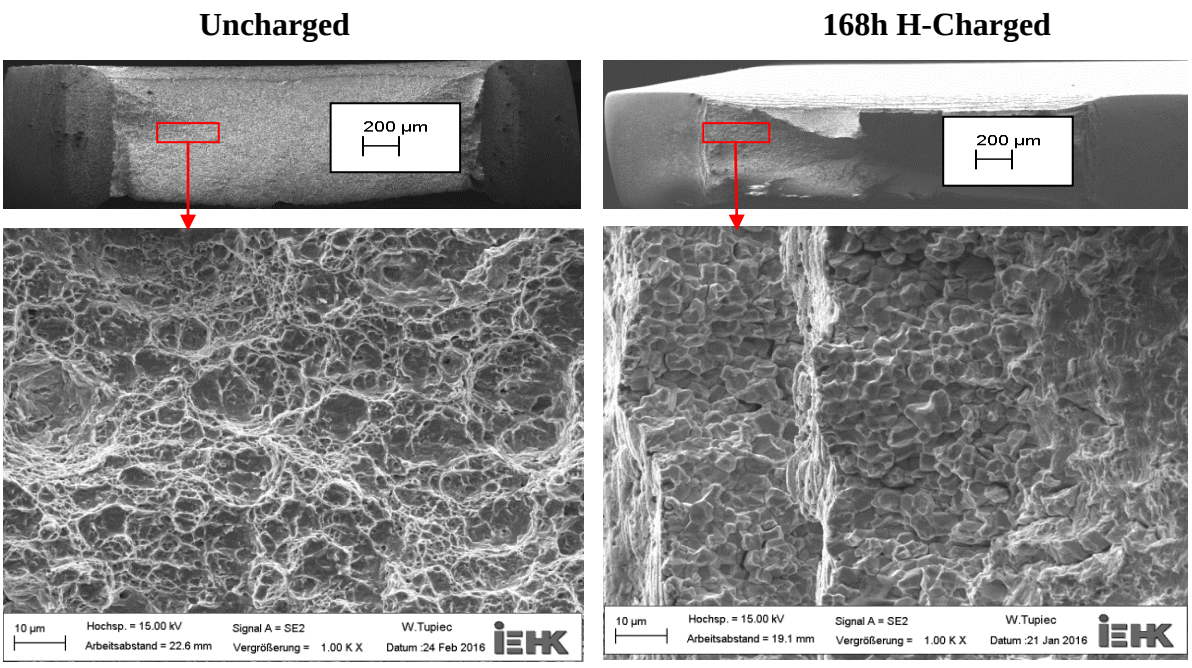

a) X60Mn22

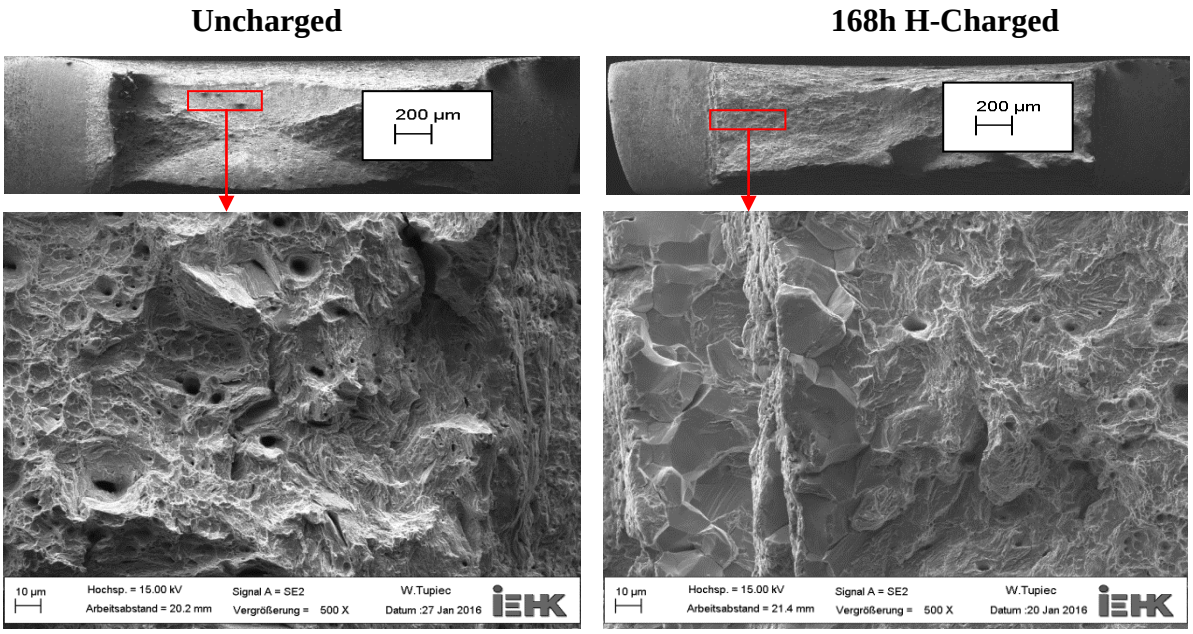

b) X30MnAl22-1

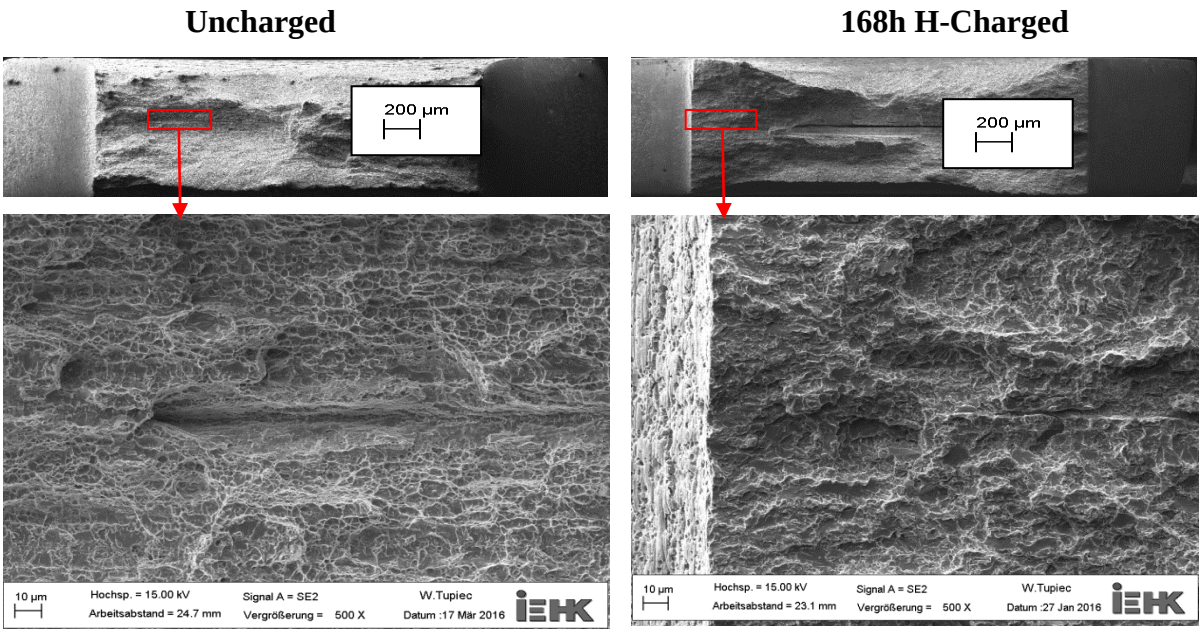

c) TRIP 800

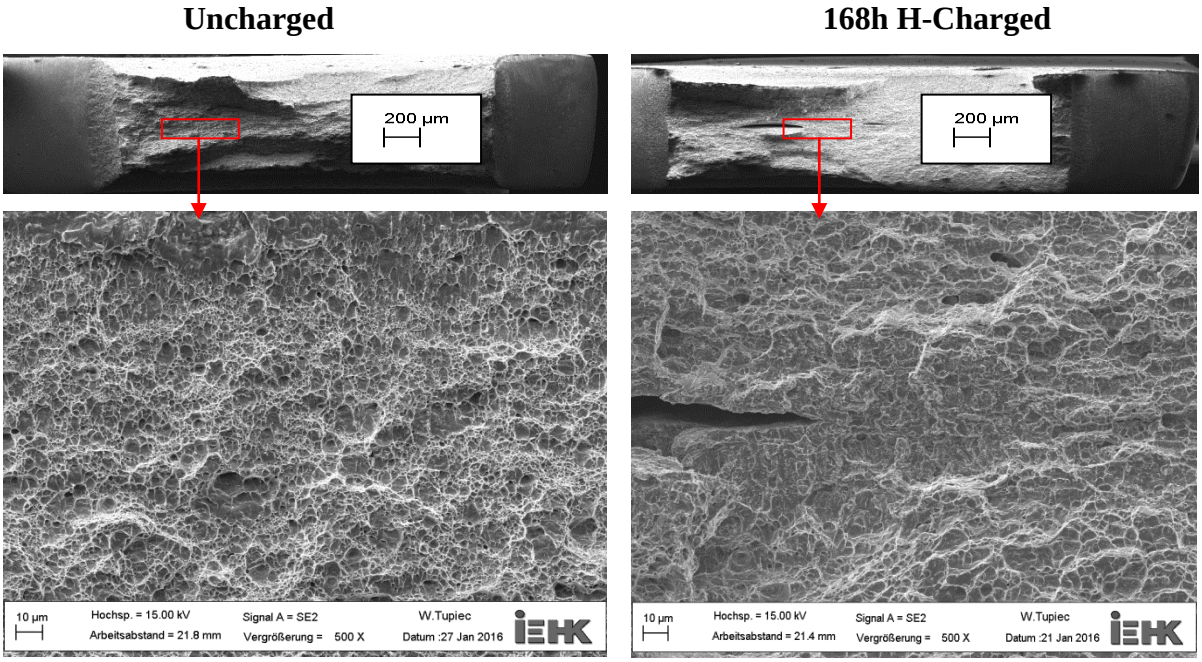

d) DP 780

Figure 5.9: SEM of the fracture surfaces of the investigated materials in uncharged and 168 hours of hydrogen charged condition after slow strain rate test.

5.2 Analysis after deep drawing

All deep drawn cups were observed to investigate the delayed fracture initiation. The process of delayed fracture initiation is recorded and the surfaces of the delayed fracture are analysed. If the blank holder force and drawing ratio are chosen correctly then Deep Drawing Tests (DDT) can be successfully performed without flange wrinkling, bottom cracking and galling. However, the successfully deep drawn cups made of delayed fracture susceptible materials, would fail after an incubation time without any external stress. The incubation time can be varied from minutes, hours or even days after deep drawing test. It depends on material susceptibility to delayed fracture.

The cracked cups show different characteristics of crack initiation and propagation, which are somehow related to their delayed fracture susceptibility. If the materials have high DF susceptibility, the crack normally initiates from rim of the cup and propagates downwards in serrated manner till it stopped growing (arrested). Cracks can initiate beneath and parallel to the arrested cracks. It is easy to understand the initiation of cracks from the cup rim, because the notches at crack rim may function as the stress riser. In addition, at the open end, crack initiation needs low free energy to concur the cohesion force of the surrounding matrix. However, if cracks initiates form the middle cup height then it is considered that it happens due to the presence of high residual stress in the deformed component. Cracks propagated in a serrated manner in the deep drawn cups.

In order to compare delayed fracture susceptibility of the as delivered materials (uncharged materials) and hydrogen pre-charged materials at the same experimental parameters, the specimens were deep drawn at blank holder force of 50 kN, punch velocity of 60 mm/min, drawing ratio of 1.8 and room temperature.

Delayed fracture in uncharged deep drawn cups of the investigated materials

Figure 5.10 showed that the as delivered materials (Uncharged deep drawn cups) of X30MnAl22-1, TRIP 800, DP 780 did not reveal any delayed fracture from the last five months after drawing at drawing ratio of 1.8. But the high manganese TWIP steel X60Mn22 showed delayed fracture after an incubation time of 60 days after DDT.

a) Cracks initiate from cup rim	b) No crack appeared from last five months	c) No crack appeared from last five months	d) No crack appeared from last five months

Figure 5.10: Delayed fracture behaviour in uncharged deep drawn cups of the investigated materials: a) X60Mn22, b) X30MnAl22-1, c) TRIP 800, d) DP 780

Delayed fracture in hydrogen pre-charged deep drawn cups of investigated materials

Figure 5.11 showed the results of deep drawing tests of the investigated materials, which were hydrogen pre-charged potentio-statically for 168 hours at -800 mV. Figure 5.11 a) showed delayed cracking behaviour in high manganese TWIP steel X60Mn22 at drawing ratio of 1.8. The crack initiated from the outer surface at crack rim after an incubation time of 24 hours. Then it propagated in a fast manner within 30 hours before slowing down. In meanwhile, others cracks initiated form other positions of the cup rim. Figure 511 b) showed that the deep drawn cup of Al-alloyed TWIP steel X30MnAl22-1 did not reveal any delayed fracture from the last four months after drawing at drawing ratio of 1.8. Figure 5.11 c) and d) showed outcome of deep drawing test of TRIP 800 and DP 780 respectively. It is clear that cup formation is not possible for TRIP and DP steel because material loses its formability due to high amount of hydrogen entered in these steels during charging because of their microstructure. Hydrogen diffusion is very fast in ferrite and martensite structure as compared to austenite structure.

a) Cracks initiate from cup rim	b) No crack appeared from last four months	c) Not able to form a cup because material loses its formability due to high amount of hydrogen	d) Not able to form a cup because material loses its formability due to high amount of hydrogen

Figure 5.11: Delayed fracture behaviour in hydrogen pre-charged (potentio-statically) deep drawn cups of the investigated materials: a) X60Mn22, b) X30MnAl22-1, c) TRIP 800, d) DP 780

Figure 5.12 showed the deep drawn cups of the investigated materials, which were hydrogen pre- charged galvano-statically for 168 hours at current density of 0.5 mA/cm^2. Figure 5.12 a), b), c) and d) showed no delayed fracture from last three months. Hence, it can be concluded that high manganese TWIP steels (X60Mn22 and X30MnAl22-1), TRIP 800 and DP 780 are resistant to delayed fracture at this condition of hydrogen charging.

a) No crack appeared from last three months	b) No crack appeared from last three months	c) No crack appeared from last three months	d) No crack appeared from last three months

Figure 5.12: Delayed fracture behaviour in hydrogen pre-charged (galvano-statically) deep drawn cups of the investigated materials: a) X60Mn22, b) X30MnAl22-1, c) TRIP 800, d) DP 780

Figure 5.13 showed the results of deep drawing tests of the investigated materials, which were hydrogen pre-charged galvano-statically for 24 hours at current density of 2.5 mA/cm^2. All the investigated materials showed the similar result at current density of 5 mA/cm^2 also. Figure 5.13 a) and b) showed no delayed cracking in high manganese TWIP steels (X60Mn22 and X30MnAl22-1) from last two months under the same experimental parameters. Figure 5.13 c) and d) showed outcome of deep drawing test of TRIP 800 and DP 780 respectively. It is clear that it is not possible to form a cup for TRIP and DP steel because material loses its formability due to high amount of hydrogen entered in these steels during charging because of their microstructure. Hydrogen diffusion is very fast in ferrite and martensite structure as compared to austenite structure.

a) No crack appeared from last two months	b) No crack appeared from last two months	c) Not able to form a cup because material loses its formability due to high amount of hydrogen	d) Not able to form a cup because material loses its formability due to high amount of hydrogen

Figure 5.13: Delayed fracture behaviour in hydrogen pre-charged (galvano-statically) deep drawn cups of the investigated materials: a) X60Mn22, b) X30MnAl22-1, c) TRIP 800, d) DP 780

5.2.1 SEM Investigation for fracture surface of deep drawn cup

Fracture surface of DDT specimens were investigated by scanning electron microscope (SEM). Among all the investigated materials, deep drawn specimens of TWIP steel X60Mn22 showed high delayed fracture susceptibility. As shown in **Figure 5.14**, the fracture surface was divided into three different regions: Crack initiation region, Middle region and Crack arrested region. From previous research work, it is known that crack propagation is characterized by three phases according to the propagation rate: the incubation time, the propagation active time and the propagation inert time.

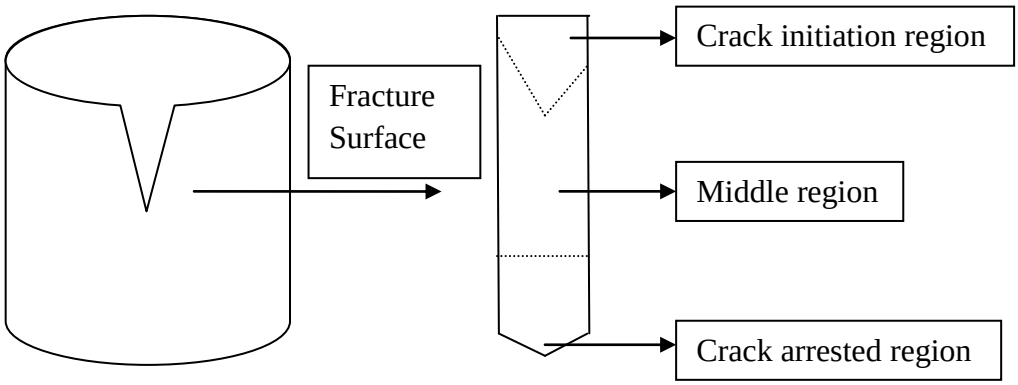

Figure 5.14: The three divided regions: Crack initiation region, Middle region and Crack arrested region, on fracture surface of deep drawn cup.

Quasi-cleavage fractures can be observed only at high hydrogen content. However, the fracture surfaces already revealed large cleavage fracture areas in deep drawn cups with low hydrogen content. **Figure 5.15,** showed the fracture surface of TWIP steel X60Mn22 in uncharged condition after deep drawing test. The cracks formed after 60 days of DDT. The cracks initiated in quasi-cleavage fracture mode from the cup rim where high tangential residual stress existed, as well as the high vertical stress resulted an extra tearing force for opening the crack. In comparison to the fracture surfaces of SSRT, the fracture surfaces of DDT specimen showed much earlier transition to cleavage fracture in the middle and arrested region when more hydrogen present in the material. As the crack propagated 6-7 mm further, the fracture surface showed mixed quasi-cleavage and cleavage fracture in the middle region. The crack growth is stopped at 15 mm from the cup rim. The full cleavage fracture mode was observed in the arrested region. Large fractions of intergranular facets were also observed in the crack-arrested region. Substantial micro cracks were observed to align with the deep drawing direction. These regions are associated with high tangential and axial residual stress where the macro cracks formed due to plastic incompatibility.

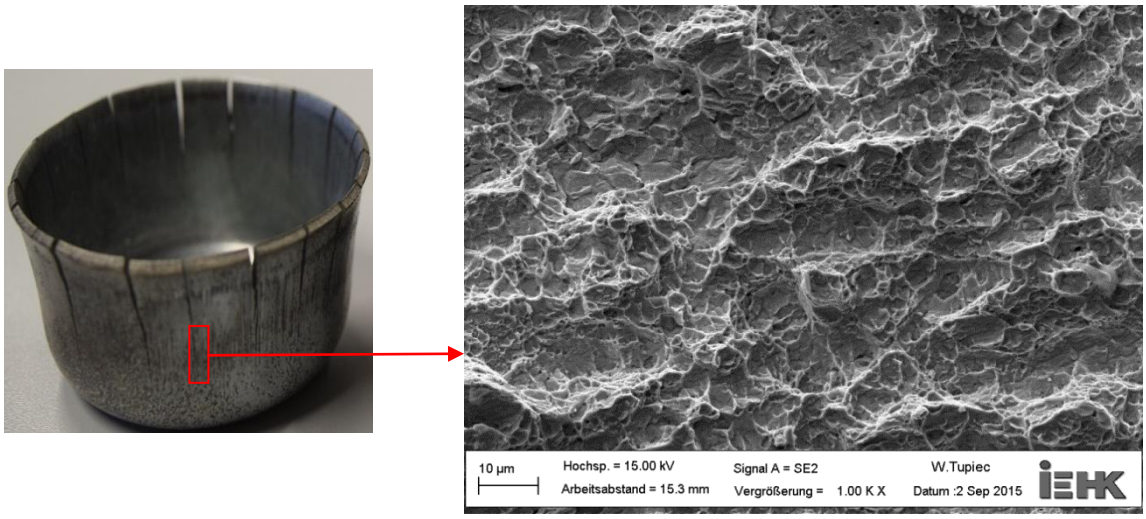

Figure 5.15: Fracture surface of TWIP steel X60Mn22 in uncharged condition after deep drawing test.

CHAPTER 6: DISCUSSION

6.1 Delayed fracture behaviour and key influencing factors in high manganese TWIP Steels, TRIP and DP Steel

The present study characterized DF behaviours in two high manganese TWIP Steels, TRIP and DP Steel. During hydrogen charging high manganese TWIP steel showed low corrosion resistance. In SSRT, hydrogen had effect on mechanical properties of X60Mn22 with high tendency to deformation twinning and high initial metallurgical hydrogen. It showed mixed fracture mode, intergranular fracture appeared as H content increased. X30MnAl22-1 showed mixed ductile and brittle fracture mode with fine AlN inclusions in dimples. In applied condition of hydrogen charging, X30MnAl22-1 did not reveal DF. Since Al alloying raises SFE and postpones deformation twinning, which leads to better DF resistance. In X60Mn22 crack initiated from cup rim with mixed ductile, transgranular and intergranular mode and arrested with intergranular mode.

During hydrogen charging TRIP and DP steel showed high corrosion resistance. In SSRT, hydrogen had great effect on mechanical properties. As the hydrogen charging hours increased, quasi-cleavage fracture appeared. In potentio-static charging, it is supposed that hydrogen content entered is very high, so TRIP and DP steel loses their formability during DDT. In galvano-static charging at current density of 0.5 mA/cm^2, TRIP and DP steel did not show delayed fracture and at higher current density, they lose their formability because of their microstructure. In TRIP and DP steel hydrogen diffusion is very fast.

In the experiments on hydrogen charging, it is observed that ferritic and martensitic structure showed very high hydrogen permeability and diffusivity compared with other austenitic structure at the same charging condition. As a result of high hydrogen diffusivity in martensitic structure, TRIP and DP steel showed high strain loss in hydrogen charged specimens. The mechanical degradation was accompanied by severe embrittlement of the fracture surface.

The investigated high manganese TWIP steel showed twinning deformation mechanism at room temperature. There was no ε-martensite observed in the TWIP steels. In SSRT, X30MnAl22-1 showed a much more postponed serrated flow in the stress-strain curves than

X60Mn22. The strong dynamic strain aging in X60Mn22 is associated with the interaction between C-Mn point defect complexes and stacking faults. The wider and lower energy stacking faults in X60Mn22 had a longer interaction with C-Mn complexes before the trailing partial restored the original stacking sequence. Hence the dynamic pinning effect exerted by the C-Mn complexes on the dislocations within the wide stacking faults led to the remarkable dynamic strain aging behaviour in X60Mn22 [58]. This discussion also indicates that X60Mn22 has a wider SF and thus lower SFE than X30MnAl22-1. The high tensile strength of X60Mn22 was due to hindrance of dislocation glide by high twinning density. X60Mn22 showed high HE-S and DF-S in the SSRT and DDT specimens. It revealed a large amount of cleavage fracture even with low hydrogen content. The brittle fracture was further enhanced by increasing the hydrogen content, showing a mixed transgranular and intergranular fracture mode. The observed phenomena revealed that the twinning formation in X60Mn22 plays an important role in causing fractures. High density of deformation twins formed during deformation induced local stress concentration, especially at the intersections of twin lamellae and grain boundaries and the intersection of multiple twin systems. Local stress concentration leads to the formation of micro voids, which then grow into micro cracks. At the same time, the diffusive hydrogen can move to the region with a high concentration of stress under the driving force of the stress gradient. When hydrogen passes through, hydrogen atoms are probably trapped at these intersections, leading to intergranular fractures. Although deformation twins also form in X30MnAl22-1 during deformation, this material exhibited excellent resistance to HE and DF at the same experimental condition. Among the investigated materials, X30MnAl22-1 is the material with high Al alloying. Park discussed about the effect of Al in raising the SFE to minimize or delay mechanical twinning in high manganese TWIP steel [59]. Consequently, the observed low DF-S in X30MnAl22-1 could be partially attributed to less mechanical twinning and thus less stress concentration.

Many studies have observed that HE occurred due to diffusive hydrogen, and irreversible hydrogen trapping sites minimize the diffusive hydrogen. However, there is no general rule regarding whether the irreversible hydrogen trapping sites are beneficial or deleterious for HE resistance. Inclusions could be beneficial hydrogen traps on the condition that they are fine and homogeneously distributed in the matrix, such as the aluminium nitrides in X30MnAl22-1. The various and fine precipitates can also be beneficial hydrogen traps, although precipitates in the investigated materials were not investigated in this study. On the opposite

hand, the coarse inclusions or clusters of inclusions are supposed to be non-beneficial traps, since they have large area of interface for hydrogen accumulation, thereby sharply reducing the surface energy between inclusions and the matrix. These inclusions are frequently micro-crack raisers. In high manganese TWIP steel, the deformation twin boundaries are considered as irreversible hydrogen trapping sites [60].

Dislocations are considered as low energy hydrogen traps compared to other lattice defects. It is proposed that hydrogen was transported with dislocation movement, when the materials are deformed at a low strain rate. In this thesis, hydrogen assisted embrittlement was most clearly revealed in the SSRT with the investigated materials. Hydrogen around moving dislocations can be captured at inclusions, twin intersections and so on. Therefore, dislocations act as a medium of transporting hydrogen to high energy hydrogen traps. At the same time, hydrogen facilitates dislocation emission, movement, and thus enhance the localized plasticity and the formation of micro voids [48]. In both cases, dislocations are non beneficial trapping sites that make hydrogen more active in the matrix.

Ab-initio calculation proposed that grain boundaries are considered a more effective hydrogen trapping medium than quick hydrogen transport channels [61,62]. Poor grain boundary properties, such as low purity, film-like carbides segregation [63] and stress concentration due to deformation twins, results in excessive hydrogen trapping and crack initiation. In present work, X60Mn22 showed intergranular fractures as hydrogen charging hours increased. .

6.2 Hydrogen Effects on Delayed Fracture

6.2.1 Deterioration of mechanical properties with increasing hydrogen charging hours

In SSRT, for all of the investigated materials, both tensile stress and tensile strain decreased with increasing hydrogen charging hours, as shown in Figure 5.1. The HE-S of the investigated materials was revealed by strain loss. This showed severe effect of hydrogen on ductility.

In DDT, X60Mn22 showed shorter incubation time to fracture due to the presence of hydrogen which is an indicator of DF-S, except in X30MnAl22-1. The reasons for the good hydrogen resistance of X30MnAl22-1 are the stable austenite structure, homogeneous deformation twinning and AlN as beneficial hydrogen traps.

In the investigated materials, the local accumulation of hydrogen at stress-concentrated regions during dynamic or static straining is assumed the main reason for degraded mechanical properties. In TRIP and DP steel, martensite plays an additive role because of low hydrogen solubility and high hydrogen diffusivity in martensite. The martensite phase acts as a quick hydrogen diffusion path and is easily embrittled. In high manganese TWIP steel, the deformation twinning generates high stress concentration at twin plate intersections or intersections with grain boundaries. Hydrogen has high affinity to these lattice imperfections and is driven to these sites under the external or residual stress gradient. These combined effects resulted in DF-S significantly. In SSRT, strain losses in specimens and in DDT, decrement in incubation time to fracture showed high crack susceptibility. However, when hydrogen content is low (1 to 3 ppm), the residual stress and stress concentration become the dominating factors. They assist microstructural defects, such as micro cracks and micro voids as well as enhance the localization and effects of hydrogen.

6.2.2 Transition of fracture mode with increasing hydrogen charging hours

The effects of hydrogen on the transition of fracture modes are described by the investigations on fracture surfaces of investigated materials. As already discussed about the influence of the microstructure on fracture mode, along with that it is found that the effects of hydrogen on fracture mode transition are different for different materials according to different mechanical tests.

In SSRT specimens, the sub-surface zone on the fracture surfaces were really affected by increasing hydrogen charging hours. The sub-surface of the fracture surfaces of X60Mn22 specimens showed mixed ductile-brittle fracture regions. This fracture mode could have resulted from the initiation of the stress-oriented fracture. This is because mechanical twins formed intensively in X60Mn22 due to its low SFE. As the hydrogen charging hours increased, the transgranular fracture regions also increased. When the material had high hydrogen content, the fracture surface showed intergranular farcture, which could have

resulted from hydrogen accumulation at grain boundaries or twin lamellae/grain boundary intersections. Recent study by Guiterrez-Urrutia et al. revealed decohesion at twin intersections or twin-grain boundary intersections by electron channeling contrast imaging (ECCI) and electron backscatter diffraction (EBSD) [15].

In TRIP and DP steel, as the hydrogen charging hours increased, the ductile dimples in the sub-surface zone gradually expanded. Fracture surfaces of TRIP and DP steels showed increasing dimple size with increasing hydrogen charging hours. The brittle feature inside the dimples was an indicator of the hydrogen-embrittled martensite phase. The cleavage facets were found inside the wall of locally expanded dimples.

In X30MnAl22-1 material, the sub-surface of the fracture surfaces in SSRT showed negligible growth of dimples size. The unaffected fracture surfaces related to the low embrittlement indexes. The fine and homogeneously distributed aluminium nitrides in material X30MnAl22-1 were supposed to freeze the diffusive hydrogen, without inducing hydrogen localization. X30MnAl22-1 has higher SFE than X60Mn22 and also showed postponed mechanical twinning. In addition, the AlN, the reduced twin lamellae/grain boundary intersections and homogeneous distribution of deformation twins also contribute to suppressing material embrittlement [64]. Moreover, as an alloy element with high passivity, Al probably increases the corrosion resistance of steels [65]. These reasons describe the low DF-S in X30MnAl22-1 and the high DF-S in X60Mn22.

Comparison of tensile (SSRT) specimens with DDT specimens showed the influence of stress tri-axiality on the fracture surfaces, which showed a general ductile mode in the tensile stress state. Quasi-cleavage fractures can be observed only at high hydrogen content. However, the fracture surfaces already revealed large cleavage fracture areas in deep drawn cups with low hydrogen content. The cracks initiated in cleavage fracture mode from the cup rim where high tangential residual stress existed, as well as the high vertical stress resulted an extra tearing force for opening the crack. In comparison to the fracture surfaces of SSRT, the fracture surfaces of DDT specimen showed much earlier transition to cleavage fracture in the middle and arrested region when more hydrogen present in the material. Substantial micro cracks were observed to align with the deep drawing direction. These regions are associated with high tangential and axial residual stress where the macro cracks formed due to plastic incompatibility. This is the main reason that influences DF at low hydrogen content.

6.3 Influences of stress and strain on hydrogen embrittlement and delayed fracture

6.3.1 Macroscopic stress and local stress concentration on crack initiation

Hydrogen has a great influence on critical fracture stress. It is found that critical fracture stress decreased with increasing hydrogen charging hours in the applied mechanical tests. However, the microscopic stresses could not be revealed and compared among different tests. In SSRT, the strain rate is kept low so that hydrogen got sufficient time for its distribution within the material. When the load is applied on specimens, inhomogeneous lattice defects lead to local stress concentration at some sites. The stress gradient between the stress concentrated region and its surroundings is the driving force for hydrogen redistribution. Local hydrogen concentration becomes higher than its surroundings, depending on the stress gradient and hydrogen molar volume. This leads to continuous transportation of hydrogen atoms to stress concentrated regions, which can further increase localized plasticity or can decrease the matrix cohesion force. Due to the combined effects of hydrogen and local stress raisers, the micro voids grow, accumulate and form micro cracks.

After DDT, deep drawn cups showed high DF-S and it also described that the induced micro cracks reduce fracture stress. In the deep drawn cups, cracks initiated and propagated easily at high hydrogen content. When a very high amount of hydrogen present in materials due to pre-charging, the time required for crack initiation and propagation is reduced. High manganese TWIP steel with strong deformation twinning are susceptible to DF. The reduction in local stress concentration and micro cracks are helpful in postponing or preventing fracture initiation.

6.3.2 Delayed fracture due to tri-axial loading

It is observed that DF-S in deep drawing specimens is much higher than that in tensile specimens. In DDT specimens, the SEM investigations of fracture surface showed mostly quasi-cleavage and intergranular fracture even at low hydrogen content. In comparison, the fracture surfaces of tensile specimens revealed substantial ductile fracture regions with same amount of hydrogen pre-charging. In DDT, deep drawn specimens are subjected to high tri-axial stress state. The specimens possess high tangential stress in the outer surface and

compressive stress in the inner surface. Maximum tri-axial tensile stress is located at the frontal sites of crack tips, where the hydrogen content first reaches its critical value [66]. The combined effects of lattice defects and hydrogen enrichment lead to the risk of catastrophic cross-linked liner failure.

6.3.3 Influences of strain rate on hydrogen embrittlement

From many literatures, it is found that most of the materials were more susceptible to HE at slow strain rate of 10^{-6}/s than at a high strain rate of 10^{-3} /s for two reasons. The first reason is the hydrogen-dislocation interaction during the deformation process. At room temperature, austenitic steel has very low hydrogen diffusivity. Hence, the transportation of hydrogen by moving dislocation is more significant than by lattice diffusion. Dislocation moves slowly at low strain rate. Furthermore, the long duration of test at stressed conditions allows time for transporting hydrogen to stress-concentrated regions or irreversible trapping sites. In contrast, at high strain rates (10^{-3} /s), which is more than five orders higher than the reported hydrogen diffusivity in the austenite microstructure, the dislocations tend to lose their hydrogen cloud during movement. The randomly distributed hydrogen is not able to reach or a very less amount of hydrogen is reached to the stress concentrated regions. Hence, the effective hydrogen diffusivity is lower. The second reason is that the high strain rate increased adiabatic heating. The heat generated during phase transformation can not dissipate at high strain rate. As a result, adiabatic heating postpones deformation twinning in high manganese TWIP steel and also suppresses martensitic transformation in other materials. HE-S was reduced by controlling the detrimental martensitic phase.

CHAPTER 7: CONCLUSIONS

The current thesis investigated delayed fracture (DF) behaviours in high manganese TWIP steels, DP and TRIP. The as delivered materials contain a little amount of hydrogen. Hydrogen can be further introduced by electrochemical hydrogen charging. Slow strain rate test (SSRT) and deep drawing test (DDT) were conducted to describe the mechanical properties and fracture behaviour as a function of hydrogen charging hours. The influence of hydrogen charging hours, crystal structure, chemical composition and lattice imperfections on DF were investigated. The loss in ductility of materials due to hydrogen is investigated by SSRT. The fracture surfaces of the materials were observed by SEM.

Effect of hydrogen on mechanical properties, fracture modes and delayed fracture

1) In SSRT, hydrogen embrittlement susceptibility (HE-S) was evaluated quantitatively by the embrittlement indexes of strain loss in the tensile specimens and complex stress state influence in the notched tensile specimens after hydrogen charging. This increased with increment of hydrogen charging hours. This indicates that hydrogen has a strong effect on material ductility.
2) In DDT, the incubation time to fracture is effective parameter for the evaluation of delayed fracture susceptibility (DF-S).
3) When a large amount of hydrogen is introduced into the material by charging, hydrogen became the dominating factor affecting the mechanical properties in SSRT and affecting the incubation time to DF in DDT. When the hydrogen content increased, the incubation time to fracture decreased from days to hours after DDT in X60Mn22.
4) TWIP steels are less susceptible to hydrogen embrittlement as compared to TRIP and DP steel.
5) When the hydrogen charging hours increased, the SEM investigation of fracture surface showed the transition of fracture mode from ductile to quasi cleavage and to the intergranular fracture mode. The transition from ductile to brittle started as the dimples expanded, indicating hydrogen enhanced localized plasticity.
6) Austenitic structure is less susceptible to hydrogen embrittlement than ferritic and martensitic structures, which is a result of high solubility and low diffusivity of

hydrogen in FCC crystal matrix. Materials with low austenite stability are susceptible to DF at low hydrogen content. However, austenite stability is not the only cause of DF resistance.

7) Delayed fracture in the Al-alloyed grade X30MnAl22-1 was fully prohibited at different charging conditions. Since Al postpones deformation twinning and enables more homogeneous twin distribution and also it increases the stacking fault energy of austenite so that the mechanical twinning is reduced, and the formation of deformation-induced martensite eliminated. It explored benefit of homogeneously dispersed fine Aluminium Nitrides as hydrogen traps that acts as an obstacle for diffusion of hydrogen in steel.
8) TRIP and DP steel did not reveal any delayed fracture in galvano-static charging at low current density but at higher current density and in potentio-static charging, they lose their formability.
9) Hydrogen-dislocation interaction is prominently increased at low strain rates so the materials tested in SSRT showed degradation of mechanical properties.

In summary, the results of this study showed the effects of hydrogen on DF behaviour in High manganese TWIP steel and other AHSS. The results showed that the complex degradation process is influenced by a bunch of interactive parameters and cannot be understood by any single mechanism. Hence, this thesis discussed the underlying factors of DF in high manganese TWIP steels, TRIP and DP steel under lean and rich hydrogen conditions separately. The results are significant for making recommendations to increase material resistance to DF by modifying material design and process control.

SCOPE FOR FUTURE WORK

The main purpose of the present thesis work is to evaluate the macroscopic effect of hydrogen on materials properties (such as to know effect of hydrogen on materials ductility, delayed fracture). The future work can be to investigate the microscopic effect of hydrogen on materials properties.

The scope for future work is given below:

1. Hydrogen content measurement can be determined by vacuum hot extraction with a hydrogen analyser model based on the carrier gas method.
2. Thermal Desorption Analysis (TDA) can be conducted to reveal the binding energy of hydrogen with different structural imperfections.
3. In-situ Transmission Electron Microscope (TEM) can be used to trace H-dislocation interaction and to reveal microscopic deformation mechanisms.
4. Electron back scatter diffraction (EBSD) can be performed to reveal the fracture propagation with respect to grain orientation, twinning plates, grain boundary, secondary phase etc.
5. The diffusion behaviour and diffusion depth of hydrogen can be determined.
6. It is assumed that residual stress which is present in materials after DDT can be one of the main causes of delayed fracture in steels. The macroscopic tangential residual stress can be determined by sectioning method. The tangential and axial residual stresses on deep drawn specimens can also be measured by X-Ray diffraction.

REFERENCES

[1] Mittal, S. C., Prasad, R. C. & Deshmukh, M. B.: Effect of hydrogen on the Impact behaviour of an austenitic Fe-Mn-Al alloy. ISIJ International 35(3) (1995), pp. 302-308.

[2] R.A. Orinai, J.P. Hirth, M. Smialowski, ed.: Hydrogen Degradation of Ferrous Alloys; Park Rodge, NJ: Noyes Publications (1985), pp. 822-862.

[3] Y. Liang, P. Sofronis, N. Aravas: On the Effect of Hydrogen on Plastic Instabilities in Metals; Acta Mater. 51 (2003), pp. 2717-2730.

[4] C. San Marchi et al.: Hydrogen Assisted Fracture of Austenitic Stainless Steels; International Hydrogen Conferences, Wyoming (2008), pp. 88-96.

[5] K.T. Park, K.G. Jin, et al. "Stacking fault energy and plastic deformation of fully austenitic high manganese steels: Effect of Al addition", Materials Science and Engineering A 527 (2010), pp. 3651–3661.

[6] K.H. So, J. S. Kim, et al.: Hydrogen Delayed fracture Properties and Internal Hydro-gen Behavior of a Fe-18Mn-1.5Al-0.6C TWIP Steel; ISIJ International, Vol. 49(2009), No. 12, pp. 1952-1959.

[7] Kwang-Geun Chin, Chung-Yun Kang, etc.: Effects of Al addition on deformation and fracture mechanisms in two high manganese TWIP steels; Materials Science and Engineering A 528 (2011), pp. 2922–2928.

[8] A. Saeed-Akbari, J. Imlau, et al., "Derivation and Variation in Composi tion-Dependent Stacking Fault Energy Maps Based on Subregular Solution Model in High-Manganese Steels", Metallurgical and Materials Transactions A, 40A (2009), pp. 3076-3090.

[9] A. Dumay, J.P. Chateau, et al.,"Influence of Addition Elements on the Stacking Fault Energy and Mechanical Properties of an Austenitic Fe-Mn-C steel", Material Science And Engineering A, 483-484 (2008), pp. 184-187.

[10] O. Grässel, L.Krüger, G. Frommeyer, L.W. Meyer: High strength Fe-Mn-(Al, Si) TRIP/TWIP steels development-properties-application, International Journalof Plasticity, 16 (2000), pp. 1391-1409.

[11] O. Bouaziz, S. Allain, C.P. Scott, P. Cugy,D. Barbier: Solid State Mater, Sci, 15 (2011), pp. 141.

[12] M. Koyama, T. Sawaguchi, K. Tsuzaki: Tetsu-to-Hagane, 98, in press.

[13] Kwansoo Chung, KanghwanAhn, Dong-Hoon Yoo, et al.: Formability of TWIP (twinning induced plasticity) automotive sheets, International Journal of Plasticity, 27 (2011), pp. 52–81.

[14] B. C. De Cooman, K.-G.Chin, J. Kim: High Mn TWIP steels for automotive applications, M. Chiaberge (Ed.), New Trends and Developments in Automotive System Engineering (2011), ISBN: pp. 978-953-307-517-4.

[15] I. Gutierrez-Urrutia, S. Zaefferer, D. Raabe: The effect of grain size and grain orientation on deformation twinning in a Fe-22 wt.% Mn-0.6 wt.% C TWIP steel, Materials Science and Engineering, A527(2010), pp. 3552-3560.

[16] Jingpei Xie, Wenyan Wang, Jiwen Li et al.: Abrasion resistant austenitic high manganese steels[M], Beijing:Science Press (2008), pp. 81-82.

[17] Ding Hao.: Microstructures, Mechanical Properties and Deformation Mechanism of High Manganese TRIP/TWIP Steels, PhD Thesis, Northeastern University (2010).

[18] Kim Young-Gil, Han Jae-kwang.: Ultra-low temperature alloy and process for manufacturing the same, US patent, 4847046 (1989).

[19] D. Canadinc, H. Sehitoglu, H. J. Maier, et al.:Strain hardening behavior of aluminum alloyed Hadfield steel single crystals[J], Acta Materialia (2005), 53: pp. 1831-1842.

[20] M.V. Biezma, The role of hydrogen in microbiologically influenced corrosion and stress corrosion cracking, International Journal of Hydrogen Energy 26 (2001), pp. 515-520.

[21] W.Y. Choo, J.Y. Lee, Metall. Trans. A 13A (1982), pp. 135–140.

[22] M. Nagumo, K. Takai, N. Okuda, J. Alloys Compd. 293-295 (1999), pp. 310–316.

[23] F.G. Wei, K. Tsuzaki, Metall. Mater. Trans. A 37A (2006), pp. 331–353.

[24] T. Tsuchida, T. Hara, K. Tsuzaki, Tetsu To Hagane 88 (2002), pp. 771–778.

[25] G.M. Evans, E.C. Rollason, J. Iron Steel Inst. (1969) 1484.

[26] Aucouturier, M. Uses of autoradiography technique for the prevention of hydrogen embrittlement of steels, through the control of microstructures. In proceedings of the first International conference on current solutions to hydrogen problems in steels, Washington Dc, November 1-5 (1982), pp. 407-412.

[27] Mishra, B., Olson, D. L. & Sanchez, F. An assessment of magnetization effects on hydrogen cracking for thick walled pipelines. Report no: CSM/MT/CWJCR (2005)/(2009) Herndon, VA: Department of metallurgical and materials engineering.

[28] Pepperhoff ,W. & Acet, M. Constitution and magnetism of iron and its alloys, Berlin Springer (2001).

[29] Gottstein, G. Physical foundations of materials science. Berlin; London: Springer (2004).

[30] Gangloff, R. P. Hydrogen assisted cracking of high strength alloys. Comprehensive Structural Integrity 6 (2003), pp. 1-194.

[31] Interrante, C.G. & Raymond, L. Hydrogen Damage. In Corrosion Tests and Standards: Application and Interpretation, 322-340 (Ed R. Baboian). West Conshohocken, PA: ASTM International (2005).

[32] R.A. Orinai, J.P. Hirth, M. Smialowski, (Eds.): Hydrogen Degradation of Ferrous Alloys, William Andrew Publishing/Noyes (1985), pp. 9,17 and 37.

[33] H. Vehoff: Hydrogen in Metals III , Springer Berlin / Heidelberg ,Chap. Hydrogen related material problem (1997) , pp. 215-274, P. 9,14,29,37 and 40.

[34] S. Lynch: Mechanisms of hydrogen assisted cracking- a review, in International conference on Hydrogen Effects on Materials Behaviour and Corrosion Deformation Interactions ,Moran, WY; USA (2002), pp. 449-466.

[35] A. Troiano: The role of hydrogen and other interstitials in the mechanical behaviour of metals, Trans. ASM 52, 54-80 (1960), pp. 37.

[36] J. Hirth: Effects of hydrogen on the properties of iron and steel, Metall. Trans. A 11A, 861-890 (1980), pp. 37.

[37] Zapffe, C. & Sims, C. Hydrogen Embrittlement, Internal Stress and Defects in Steel. Transaction AIME 145 (1941), pp. 225-229.

[38] I. M. Robertson, D. Teter: Controlled environment transmission electron microscopy, J. Microsc. Res. Tech. 42,260 (1998), pp. 29,30,34,37 and 40.

[39] D. F. Teter, I. M. Robertson, H. K. Birnbaum: The effects of hydrogen on the deformation and fracture of β-titanium, Acta Mater. 49,4313-4323 (2001). pp. 29,30,34,37 and 40.

[40] B. Makenas, H. Birnbaum: Phase changes in the niobium-hydrogen system. I.-accommodation effects during hydride precipitation, Acta Metall. 28,979-988 (1980), pp. 37.

[41] D.G. Westlake, A generalized model for hydrogen embrittlement, Trans ASM, 62 (1969), pp. 1000 – 1006.

[42] H.K. Birnbaum, Mechanisms of hydrogen related fracture of metals, Hydrogen effects on materials behavior, N.R. Moody and A.W Thompson (Eds), TMS (1990), pp. 639 – 658.

[43] H.K. Birnbaum, I.M. Robertson, P. Sofronis, and D. Teter, Mechanisms of hydrogen related fracture – a review, Corrosion-deformation interactions, T. Magnin (Ed.), Inst. of Mat. (1997), pp. 172-195.

[44] Barnoush, A., Hydrogen embrittlement, revisited by in situ electrochemical nanoindentation. In Materials Science and Methods, Vol. PHD thesis, 288 Saarbrucken: Saarland University, Germany (2007).

[45] Ćwiek, C. & Zieliński, A., Mechanism of hydrogen enhanced-cracking of high-strength steel welded joints. Journal of Achievements in Materials and Manufacturing Engineering 18(1-2) (2006), pp. 207-210.

[46] J. Eastman, T. Matsumoto, N. Narita, F. Heubaum and H. K. Birnbaum, in I. M. Bernstein and A.W. Thompson (eds.), Hydrogen in Metals, TMS, New York (1980), pp. 397.

[47] T. Matsumoto, J. Eastman and H. K. Birnbaum, Scripta Metall., 15 (1981) 1033.

[48] Birnbaum, H. K. & Sofronis, P., Hydrogen-enhanced localized plasticity-A mechanism for hydrogen-related fracture. Materials Science and Engineering: A 176(1-2) (1994), pp. 191-202.

[49] Nagumo, M., Function of hydrogen in embrittlement of high-strength steels. ISIJ International 41(2001): pp. 590-598.

[50] C. J. Mc Mahon: Hydrohen-induced intergranular fracture of steels, Eng. Fract. Mech. 68,773-788 (2001), pp. 37.

[51] R. Oriani: A mechanistic theory of hydrogen embrittlement of steels, Ber. Bunsenges. Phys. Chem 76, 848-857 (1972), pp. 37 and 38.

[52] Bleck, W., Frehn, A., Ratte, E., Schedin, E., Staubwasser, L., Avendano, J. L., Akdut, N., Brasseur, E., Karjalainen, P. & Juntunen, P.: Methods of improving the deep drawing properties of austenitic stainless steels Luxembourg: European Commission (2006).

[53] K.T. Park, K.G. Jin, et al. “Stacking fault energy and plastic deformation of fully austenitic high manganese steels: Effect of Al addition”, Materials Science and Engineering A 527 (2010), pp. 3651–3661.

[54] K.H. So, J. S. Kim, et al.: Hydrogen Delayed fracture Properties and Internal Hydrogen Behavior of a Fe-18Mn-1.5Al-0.6C TWIP Steel; ISIJ International, Vol. 49(2009), No. 12, pp. 1952-1959.

[55] A. Saeed-Akbari, J. Imlau, et al., “Derivation and Variation in Composition-Dependent Stacking Fault Energy Maps Based on Subregular Solution Model in High-Manganese Steels”, Metallurgical and Materials Transactions A, 40A (2009), pp. 3076- 3090.

[56] A. Dumay, J.P. Chateau, et al.,“Influence of Addition Elements on the Stacking Fault Energy and Mechanical Properties of an Austenitic Fe-Mn-C steel”, Material Science And Engineering A, 483-484 (2008), pp. 184-187.

[57] R.E. Schramm, R. Reed, “Stacking Fault Energies of Seven Commercial Austenitic Stainless Steels”, Metallurgical Transactions, 6A (1975), no.7, pp. 1345-1351.

[58] Kim, J., Lee, S.-J. & De Cooman, B. C. : Effect of Al on the stacking fault energy of Fe-18Mn-0.6C twinning induced plasticity. Scripta Materialia 65(4) (2011), pp. 363-366.

[59] Park, K.-T., Jin, K.G., Han, S. H., Hwang, S. W., Choi, K. & Lee, C. S. : Stacking fault energy and plastic deformation of fully austenitic high manganese steels: Effect of Al addition. Materials Science and Engineering: A 527(16-17) (2010), pp. 3651-3661.

[60] So, K. H., Kim, J. S., Chun, Y. S., Park, K.-T., Lee. Y.-K. & Lee, C. S. : Hydrogen Delayed Fracture Properties and Internal Hydrogen Behaviour of a Fe-18Mn-1.5Al-0.6C TWIP Steel. ISIJ International 49(12) (2009), pp. 1952-1959.

[61] Du, Y. A., Ismer, L., Rogal, J., Hickel, T., Neugebauer, J. & Drautz, R., First-principles study on the interaction of H interstitials with grain boundaries in α and γ-Fe. Physical Review B84(144121) (2011).

[62] Von Pezold, J., Lymperakis, L. & Neugebeauer, J. : Hydrogen-enhanced local plasticity at dilute bulk H concentrations: The role of H-H interactions and the formation of local hydrides. Acta Materialia 59(8) (2011), pp. 2969-2980.

[63] Kim, J., Lee, Y. H., Lee, D. L., Park, K.-T. & Lee, C. S. : Microstructural influences on hydrogen delayed fracture of high strength steels. Materials Science and Engineering: A 505 (2009), pp. 105-110.

[64] Chin, K.-G., Kang, C.-Y., Shin, S. Y., Hong, S., Lee, S., Kim, H. S., Kim, K.-h. & Kim, N. J. : Effects of Al addition on deformation and fracture mechanisms in two high manganese TWIP steels. Materials Science and Engineering : A 528(6) (2011), pp. 2922-2928.

[65] De Cooman , B. C., Chin, K.-g. & Kim, J. : High Manganese TWIP Steels for Automotive Applications. In New Trends and Developments in Automotive System Engineering (Ed M. Chiaberge). Rijeka, Croatia: InTech (2011), pp. 109-110.

[66] Zhao, M., Liu, M., Atrens, A., Shan, Y. & Yang, K. : Effect of applied stress and microstructure on sulfide stress cracking resistance of pipeline steel subject to hydrogen sulfide. Materials Science and Engineering: A 478 (2008), pp. 43-47.

[67] A. Laureys, T. Depover, R. Petrov, K. Verbeken: Characterization of hydrogen induced cracking in TRIP-assisted steels, Int. J. Hydrog. Energy 40 (2015), pp.169–175.